PHYSICAL REVIEW C VOLUME 21, NUMBER 4 APRIL 1980

Hartree-Fock-Bogolyubov calculations with the $D1$ effective interaction on spherical nuclei

J. Dechargé and D. Gogny
Service de Physique Neutronique et Nucléaire, Centre d'Etudes de Bruyères-le-Châtel, Boîte Postale No. 561, 92542 Montrouge Cedex, France
(Received 3 August 1979)

A self-consistent approach allowing the introduction of pairing into a comprehensive study of the bulk as well as the structure properties of nuclei is presented. It is emphasized that the density-dependent effective force used in the calculations reported here does permit the extraction of the mean field and the pairing field in the framework of the Bogolyubov theory. First, a brief review of Hartree-Fock-Bogolyubov formalism with density-dependent interactions is presented. Then the derivation of the effective interaction is explained and some details concerning the nuclear matter properties are given. Finally, we report the studies on spherical nuclei with special reference to the pairing properties. In order to demonstrate the versatility of our approach a comprehensive study of various nuclear properties is given. In view of the abundance of results obtained with our approach we plan to report the results on the deformed nuclei in a future publication.

[NUCLEAR STRUCTURE Density-dependent Hartree-Fock-Bogolyubov (DDHFB) approximation applied to the calculations of the structure of spherical nuclei: binding energies, pairing correlations, density distributions, magnetic form factors, and quasiparticle spectra.]

I. INTRODUCTION

This paper is devoted to the description of a self-consistent approach which takes into account the pairing correlations between like particles. Our approach is essentially based on the density-dependent Hartree-Fock theory (DDHF) with a phenomenological interaction. In order to better place the present work we refer the reader to the other papers,[1-4] where the status of the several attempts to derive the average field in nuclei has been reviewed in detail. See also the review of the DDHF calculations given by Bethe.[5] Let us recall the general idea governing the DDHF theory since our approach is its direct extension. One assumes some predetermined parametrization of the effective force between two nucleons and defines the total energy of the system in the usual way, i.e., as the sum of the total kinetic energy plus the potential energy calculated with that force. In this way one obtains an explicit functional of the one- and the two-body density matrices which reduce to an expression in terms of the one-body density matrix when the wave function of the system considered is described by a Slater determinant. Then one applies the variational principle in order to determine the equilibrium density corresponding to the ground state of the system which provides Hartree-Fock-type equations and defines at the same time the average field in the system. This procedure is somewhat arbitrary since there is no rigorous argument justifying the use of the variational principle with an effective force.[6] In fact, one follows the procedure of the more fundamental approach starting with a Brueckner G matrix where the average field is extracted from the variation of the lowest-order approximation to the energy.[7,8] There one finds a justification for this procedure by the fact that it introduces in the definition of the average field important classes of diagrams which are seen *a posteriori* to play an important role in the calculation of the saturation properties. In the phenomenological DDHF theory it is equivalent to saying that—via the rearrangement terms occurring in the definition of the Hartree-Fock (HF) field—this procedure modifies the usual HF relation between the single particle energies and the binding energy. This modification makes it possible to adjust the global properties (radii, binding energies) as well as to obtain a sufficiently compressed single particle spectrum.

Concerning the phenomenological effective interaction, its parametrization differs according to different authors. Some of them introduce an explicit dependence on the density.[9-12] Others introduce the three-body contact force of Skyrme which is equivalent to a linear dependence on the density in the HF calculations when spins are saturated. All of them neglect possible energy dependence for the sake of simplicity. Such direct parametrizations have the advantage of rendering the extensive calculation simpler. The various applications presented by the Orsay group with the Skyrme's force give a clear indica-

tion of the possibilities offered by this approach. However, the disadvantage of this phenomenology is that we have no link with any perturbation theory allowing calculation of possible higher-order corrections. Nevertheless, we believe that there are still in this context several reasonable extensions beyond the mean field approximation, one of them being the approach we shall discuss below. In order to include pairing correlations one can generalize the DDHF theory by describing the system with an independent quasiparticle wave function, the quasiparticles being defined via the general Bogolyubov transformation. Thus the total energy of the system becomes a functional not only of the density matrix but also of a new object called the pairing tensor. Again applying the variational principle one generalizes the Bogolyubov equations with density-dependent effective forces. From now on we shall denote this approach as density-dependent Hartree-Fock-Bogolyubov theory (DDHFB). In the past there have been performed several interesting Hartree-Fock-Bogolyubov (HFB) studies on light nuclei of the (s,d) and (p,f) shells,[13-15] but one may wonder if the effective density-independent forces they employed have the properties required to treat on the same footing the average and the pairing field. In fact, if one refers to the simple BCS picture using the HF basis one knows the important role played by the single particle spectrum and in particular by the HF gap. It is only since the advent of the density-dependent forces that one gets reasonable single particle spectrum (not too large a HF gap and reasonable level density around the Fermi sea), and it seems to us that the DDHFB approach is indispensable if one desires a complete self-consistent theory of the pairing. We do not wish to refute the other approaches[16-18] which leave out the complete self-consistence but which attempt to follow closely the HFB theory in order to study the pairing effects in specific spectroscopic problems. However, we want to stress the different advantages of a self-contained approach. As we explain below, the effective force is determined once and for all and we can carry out systematic calculations on spherical and deformed nuclei even in the region where nothing is known experimentally. On the other hand, it can be extended to the theory of the collective motions of large or small amplitude associated to the fluctuations of the generalized density matrix. Thus in the same theoretical framework with no other parameters than those included in the effective interaction, one describes the single quasiparticle excitations together with the collective excitations of the average and the pairing field.

In view of the abundance of results we have obtained with the DDHFB theory and the success of this approach in reproducing a great variety of nuclear properties, we shall present its various aspects in a series of papers. In this paper we present the results concerning the spherical nuclei. In the first part we describe the DDHFB formalism for the systems with an even number of nucleons and specialize the Bogolyubov equations to the spherical symmetry. We present also the way we treat the systems with an odd number of nucleons so as to establish the connection of the theory with experimental data. In the second part we explain the derivation of the interaction and give in detail its properties in the nuclear matter. We discuss also the necessity of using an effective force of nonzero range. In the third part we report on the studies of spherical nuclei concerning the pairing properties. Finally, in order to emphasize the versatility of our approach, a comprehensive study of various nuclear properties is given in Sec. IV.

II. HARTREE-FOCK-BOGOLYUBOV FORMALISM WITH DENSITY-DEPENDENT INTERACTION

A. The Hartree-Fock-Bogolyubov equations

Although the HFB theory was developed by different authors with various interactions, we present here briefly the formalism since the use of a density-dependent interaction leads to some modifications. This section is also necessary in order to clarify the notations and the relevant physical quantities to be discussed in the next sections.

Once the concept of the quasiparticle (QP) is introduced, the HFB theory is a direct generalization of the HF theory. In the second quantization the QP creation and destruction operators ($\eta^\dagger$ and η, respectively) are given by the most general linear transformation between the operators $a_\alpha^\dagger$ and a_α associated with an arbitrary complete basis $|\alpha\rangle$:

$$\eta_i^\dagger = \sum_\alpha u_{i\alpha}^* a_\alpha^\dagger + v_{i\alpha}^* a_\alpha ,$$

$$\eta_i = \sum_\alpha u_{i\alpha} a_\alpha + v_{i\alpha} a_\alpha^\dagger .$$

In the following we conveniently define the column vectors:

$$\eta = \begin{pmatrix} \vdots \\ \eta_i \\ \vdots \\ \eta_i^\dagger \\ \vdots \end{pmatrix}, \quad A = \begin{pmatrix} \vdots \\ a_\alpha \\ \vdots \\ a_\alpha^\dagger \\ \vdots \end{pmatrix}.$$

Then the Bogolyubov transformation reads $\eta = BA$, where in terms of the supermatrices U and V, the matrix B takes the form

$$B = \begin{pmatrix} U & V \\ V^* & U^* \end{pmatrix}.$$

The anticommutation relations between the QP operators are preserved by assuming the unitarity of B. At this stage we introduce the generalized density matrix $R = I - \langle \tilde{0} | AA^\dagger | \tilde{0} \rangle$. The product $AA^\dagger$ is interpreted as the product of a row matrix by a column matrix. The matrix R is related to the two types of contractions $\rho_{\alpha\beta} = \langle \tilde{0} | a_\beta^\dagger a_\alpha | \tilde{0} \rangle$ and $\kappa_{\alpha\beta} = \langle \tilde{0} | a_\alpha a_\beta | \tilde{0} \rangle$ which represent the density matrix and the pairing tensor. With obvious notations (Appendix C) we have

$$R^{11} = \rho, \quad R^{22} = 1 - \rho^*, \quad R^{12} = -\kappa, \quad R^{21} = \kappa^*.$$

In the HFB theory, $| \tilde{0} \rangle$ is assumed to be the QP vacuum. As a consequence, the Bogolyubov transformation B diagonalizes R ($BRB^\dagger = I - \langle \tilde{0} | \eta\eta^\dagger | \tilde{0} \rangle$) and in that particular representation it is easy to show that R corresponds to a projector ($R^2 = R$). Conversely, the condition $R^2 = R$ guarantees that $| \tilde{0} \rangle$ is an independent QP wave function. These few preliminaries facilitate the derivation of the HFB equations. In fact, the total energy $\langle \tilde{0} | H | \tilde{0} \rangle$ is expressed in terms of the matrix elements of R and minimized with respect to their variations.[19] For the reason given above one adds the subsidiary condition $R^2 = R$ and also the constraint that the average number of protons and neutrons corresponds to the given number of particles in the system. Introducing the Lagrange parameters λ_p, λ_n and Λ (Λ is an Hermitian matrix) and using the notation,

$$\mathcal{E} = \langle \tilde{0} | H - \lambda_p \hat{N}_p - \lambda_n \hat{N}_n | \tilde{0} \rangle .$$

The quantity to minimize is $\mathcal{E} - \mathrm{tr}\Lambda(R^2 - R)$ and the corresponding variational principle reads

$$\delta\mathcal{E} - \mathrm{tr}(R\Lambda + \Lambda R - \Lambda)\delta R = 0 ,$$

which, after having eliminated Λ by means of the condition $R^2 = R$, leads to

$$[\mathcal{H}, R] = 0 . \tag{1}$$

$\mathcal{H}$ stands for the Bogolyubov Hamiltonian

$$\mathcal{H} = \begin{vmatrix} \mathcal{H}^{11} & \mathcal{H}^{12} \\ \mathcal{H}^{21} & \mathcal{H}^{22} \end{vmatrix},$$

whose matrix elements are related to the derivative of the energy according to the equation

$$\mathcal{H}^{ij}_{\alpha\beta} = 2\frac{\partial \mathcal{E}}{\partial R^{ji}_{\beta\alpha}} . \tag{2}$$

The factor 2 is introduced for convenience as will be seen in what follows.

At this point it is worth stressing that the density-dependent (DD) interactions allow only calculation of the interaction energy of the system, but strictly speaking, they do not provide a Hamiltonian. In particular, the method of elimination of the dangerous diagrams, commonly used to derive the HFB equations, is not equivalent to the variational method in our case. In order to express the derivatives in the definition (2) we calculate the average value $\langle \tilde{0} | T + V(\rho) | \tilde{0} \rangle$, where $V(\rho)$ is considered as a two-body force. We get for $\mathcal{E}$,

$$\mathcal{E} = \tfrac{1}{2}\Big\{ \sum [(T_{\alpha\beta} - \lambda_{q\alpha}\delta_{\alpha\beta})\rho_{\beta\alpha} + (T_{\alpha\beta} - \lambda_{q\alpha}\delta_{\alpha\beta})^*\rho^*_{\beta\alpha}] + \tfrac{1}{2}\sum (V_{\alpha\beta\gamma\delta}\rho_{\delta\beta}\rho_{\gamma\alpha} + V^*_{\alpha\beta\gamma\delta}\rho^*_{\delta\beta}\rho^*_{\gamma\alpha})\Big\} + \tfrac{1}{4}\sum V_{\alpha\beta\gamma\delta}\kappa_{\delta\gamma}\kappa^*_{\beta\alpha} .$$

In this expression $V_{\alpha\beta\gamma\delta}$ is antisymmetrized with respect to the exchange ($\alpha \rightleftarrows \beta$), ($\gamma \rightleftarrows \delta$) and the energy is symmetrized with respect to ρ, ρ^* and κ, κ^* since these quantities are considered as independent variables. Thus with these definitions, the matrix elements $\mathcal{H}^{ij}_{\alpha\beta}$ take the form

$$\mathcal{H}^{11} = T - \Lambda + \Gamma = e , \quad \mathcal{H}^{12} = \Delta ,$$

$$\mathcal{H}^{21} = -\Delta^* , \quad \mathcal{H}^{22} = -\mathcal{H}^{11*} .$$

The quantity Γ represents the HF field

$$\Gamma_{\alpha\gamma}=\sum_{\delta\beta}V_{\alpha\beta\gamma\delta}\rho_{\delta\beta}+\tfrac{1}{2}\sum_{\rho\beta\sigma\delta}\left\langle\sigma\beta\left|\frac{\partial V}{\partial\rho_{\gamma\alpha}}\right|\rho\delta\right\rangle \times(\rho_{\delta\beta}\rho_{\rho\sigma}+\tfrac{1}{2}\kappa_{\delta\rho}\kappa^{*}_{\beta\alpha}),$$

which is reduced to its usual form in the case of vanishing pairing correlations. On the other hand, the use of a DD force does not change the definition of the pairing field Δ:

$$\Delta_{\alpha\beta}=\tfrac{1}{2}\sum_{\gamma\delta}V_{\alpha\beta\gamma\delta}\kappa_{\delta\gamma}\,.$$

To complete this expression we recall that since the interaction depends only on the spatial density $\rho(\vec{r})$ we can simply calculate $\partial V/\partial\rho_{\gamma\alpha}$ as

$$\frac{\partial V}{\partial\rho_{\gamma\alpha}}=\frac{\partial V}{\partial\rho}\frac{\partial\rho}{\partial\rho_{\gamma\alpha}}=\psi^{*}_{\alpha}(r)\psi_{\gamma}(r)\frac{\partial V}{\partial\rho}\,.$$

For the solution of Eq. (1) an elegant mathematical method based on the antilinear operators was formulated.[20] It has the advantage of reducing the number of dimensions but also requires much work from a computational point of view. Thus we adopt the usual way, i.e., we note that $\mathcal{H}^{12}=\mathcal{H}^{21}=0$ in the representation diagonalizing R or equivalently that $\mathcal{H}$ does not connect the ground state to the two QP states. Consequently, we can satisfy Eq. (1) by a choice of the Bogolyubov transformation diagonalizing $\mathcal{H}$:

$$\mathcal{H}B^{\dagger}=B^{\dagger}\mathcal{E}\,.$$

This nonlinear eigenvalue problem is then solved by an iterative procedure explained below.

For the sake of completeness we express the stability condition in the case of a density-dependent interaction. Up to the second order we expand the generalized density matrix around the equilibrium density ${}^{(0)}R$:

$$R={}^{(0)}R+{}^{(1)}R+{}^{(2)}R$$

with the condition $R^2=R$. This conditions expressed in the QP representation diagonalizing ${}^{(0)}R$ leads to the relations

$${}^{(1)}R^{ii}=0\,,\quad i=1,2\,,$$

$${}^{(2)}R^{ii}=(-)^{i+1}[{}^{(1)}R{}^{(1)}R]^{ii}\,,\quad i=1,2\,.$$

On account of the stationarity condition $\mathrm{tr}(\mathcal{H}^{(0)(1)}R)=0$, the corresponding expansion for the energy is

$$E=E(\rho^{(0)}\kappa^{(0)}+\tfrac{1}{2}\mathrm{tr}_1\Big\{\mathcal{H}_1^{(0)(2)}R_1+\tfrac{1}{2}\mathrm{tr}_2\frac{\partial^2E}{\partial^{(1)}R_1\partial^{(1)}R_2}{}^{(1)}R_2{}^{(1)}R_1\Big\}\,, \tag{3}$$

where

$$E(\rho^{(0)}\kappa^{(0)})=\mathrm{tr}[T+\tfrac{1}{2}\Gamma(\rho^{(0)})]\rho^{(0)}+\tfrac{1}{2}\mathrm{tr}(\Delta^{(0)}\kappa^{(0)*})$$

is the total binding energy. If the HFB solution is to be stable, the above quadratic form must be positive for any choice of ${}^{(1)}R$. Finally, the usual quantization which consists of looking at the matrix elements of ${}^{(1)}R$ as boson operators provides the Hamiltonian associated with the fluctuations of the generalized density matrix around the HFB equilibrium. The second derivative of E is then interpreted as the residual interaction between QP. As compared to the conventional calculations this residual interaction contains the so called rearrangement terms which were shown elsewhere[21] to play an important role. In concluding this section we see that effective DD interactions provide a self-consistent scheme of single QP excitations as well as the collective excitations, despite the fact that DD forces do not provide us with a Hamiltonian.

B. Reduction of the HFB equations with the assumption of spherical symmetry

From now on we assume that the HFB Hamiltonian is invariant with respect to rotations in the coordinate and spin spaces. We also assume the reflexion symmetry. In the HFB theory these symmetries can be shown to be compatible with any number of particles. On the other hand, we treat separately the pairing correlations between the neutrons and the protons. As a consequence the QP states can be labeled by an index α which stands for the following quantum numbers: the charge quantum number q, the orbital angular momentum l, the total angular momentum j, and the magnetic quantum number m. Another index i is needed to distinguish between QP states having the same $\alpha=(q,l,j,m)$ but differing in radial quantum number.

The Bogolyubov transformation is reduced to the form

$$\eta_{i\alpha}=\sum_n u^{\alpha}_{in}a_{n\alpha}+v^{\alpha}_{in}a^{\dagger}_{n\bar{\alpha}}\,,\quad\bar{\alpha}=(q,l,j,-m)\,. \tag{4}$$

The summation is performed over the radial quantum number n. The operators $a^{\dagger}_{n\alpha}$ are associated with the functions:

$$\langle\bar{x}\,\sigma|\,a^{\dagger}_{n\alpha}|\,0\rangle=\varphi_{nl}(r)(Y_l\times\chi^{1/2})^{j}_{m}\,,$$

where $\chi_{m_s}{}^{1/2}$ denote the spin functions and Y_{lm_l} the usual spherical harmonics. In the present calculation we choose the spherical harmonic oscillator eigenfunctions for the radial part $\varphi_{nl}(r)$. Finally, using the property that the QP operators η must transform like irreducible tensors, it can be shown that u^{α}'s are independent of m while v^{α}'s depend on m via a trivial phase factor $s_{jm}=(-)^{j-m}$. The Bogolyubov transformation is then rewritten as

$$\eta_{i\alpha} = \sum_n u_{in}^{(a)} a_{n\alpha} + s_{jm} v_{in}^{(a)} a_{n\bar{\alpha}}^{\dagger} \quad (a) = (q, l, j) .$$

According to this transformation the density matrix becomes diagonal in quantum numbers (l, j, m, q) and independent of m whereas the matrix elements of the pairing tensor vanish except between the time reversed states and depend on m only via the phase s_{jm}:

$$\rho_{n\alpha;n'\beta} = \delta_{\alpha\beta} \rho_{n,n'}^{(a)} ,$$

$$\kappa_{n\alpha;n'\beta} = \delta_{\alpha\bar{\beta}} s_{j_\alpha m_\alpha} \kappa_{n,n'}^{(a)} .$$

In terms of the coefficients U and V the matrices $\rho^{(a)}$ and $\kappa^{(a)}$ have the form

$$\rho_{n,n'}^{(a)} = (V^{\dagger} V)_{nn'}^{(a)}, \quad \kappa_{n,n'}^{(a)} = (U^{\dagger} V)_{nn'}^{(a)} .$$

Conversely such selection rules on ρ and κ lead to HFB equations split with respect to the quantum number $a = (l, j, q)$ and independent of m, i.e.,

$$\begin{bmatrix} e^{(a)} & -\Delta^{(a)} \\ -\Delta^{(a)} & -e^{(a)} \end{bmatrix} \begin{bmatrix} U^{(a)} \\ V^{(a)} \end{bmatrix} = \begin{bmatrix} U^{(a)} \\ V^{(a)} \end{bmatrix} \epsilon^{(a)} ,$$

where $\Delta^{(a)}$ and the pairing field $\Delta_{\alpha\beta}$ are related via the equation

$$\Delta_{\alpha\beta} = \delta_{\alpha\bar{\beta}} s_{j_\alpha \bar{m}_\alpha} \Delta^{(a)} .$$

This is what was meant at the beginning of this section by the phrase: "The symmetry is compatible with any number of particles."

C. Derivation of the HF and the pairing fields

The main technical difficulty we have encountered in solving the HFB equations was to calculate with a minimum of computational time the HF and the pairing field. This difficulty is due to our interaction which contains a finite range part. We sketch briefly how we have proceeded in order to simplify maximally the calculation of these quantities. First we consider the case of the HF field. In the coordinate representation it decomposes itself into a local $\Gamma^L(r_1, r_2)$ and a nonlocal part $\Gamma^E(r_1, r_2)$. The local part takes a very simple form since all the geometry disappears, and only the lowest multipole of the interactions occurs:

$$\langle r_1 | \Gamma^L | r_2 \rangle = \delta(\bar{r}_1 - \bar{r}_2) \sum_{q'} \int V_{(0s)_0}^{qq'}(r_1, r') \rho^{q'}(r') r'^2 dr' .$$

The definition of the multipoles $V_{(ks)_p}^{qq'}$ is given in Appendix A and $\rho^{(q)}$ is the spatial density:

$$\rho^{(q)}(r) = \frac{1}{4\pi} \sum_{nn'lj} \hat{j}^2 \rho_{nn'}^{(a)} \varphi_{nl}(r) \varphi_{n'l}(r) ,$$

with

$$\hat{j} = (2j+1)^{1/2} .$$

As for the nonlocal field, except for a $3j$ coefficient which still remains, all the geometry has been reduced along the line described in Appendix B. In writing the expression $\Gamma^E(r_1, r_2)$ we define the quantities $\Theta^{lkq}(r_1, r_2)$ and $\Lambda^{lkq}(r_1 r_2)$:

$$\Theta^{lkq}(r_1 r_2) = \frac{\hat{k}^2}{4\pi} \sum_{l'nn'} \begin{pmatrix} l & k & l' \\ 0 & 0 & 0 \end{pmatrix}^2 \varphi_{nl}(r_1) \varphi_{n'l'}(r_2) \times [(l'+1) \rho_{nn'}^{(a)'\dagger} + l' \rho_{nn'}^{(a)'-}] \quad (5)$$

and

$$\Lambda^{lkq}(r_1 r_2) = \frac{\hat{k}^2}{4\pi \bar{l}} \sum_{\substack{l' \neq 0 \\ nn'}} \begin{pmatrix} l & k & l' \\ 0 & 0 & 0 \end{pmatrix}^2 \frac{(\bar{l} + \bar{l}' - \bar{k})}{\bar{l}'} \times (\rho_{nn'}^{(a)'+} - \rho_{nn'}^{(a)'-}) \varphi_{nl}(r_1) \varphi_{n'l'}(r_2) . \quad (6)$$

We use the notations

$$(a)'\pm = (l', l' \pm \tfrac{1}{2}, q) ,$$

$$\bar{l} = l(l+1) ,$$

$$\hat{k} = (2k+1)^{1/2} .$$

In the case $l = 0$, Λ must be taken equal to zero. With these definitions the nonlocal HF field becomes

$$\Gamma^{E(a)}(r_1, r_2) = \sum_{kq'} \{[V_{k0}^{qq'}(r_1 r_2) + 3V_{k1}^{qq'}(r_1 r_2)]/2\} \Theta^{lkq'}(r_1 r_2) + \langle lj | \bar{l}\bar{s} | lj \rangle \sum_{kq'} [V_{k0}^{qq'}(r_1 r_2) - V_{k1}^{lkq'}(r_1 r_2)] \Lambda_{(r_1 r_2)}^{lkq'} .$$

In addition to its relative simplicity this expression has also the advantage of showing clearly how the central part of the two-body interaction contributes to the spin orbit splitting of the HF levels.

Concerning the pairing field it is clear from its definition that it must be purely nonlocal. Replacing the density matrix ρ by the pairing tensor κ in the two quantities $\Theta^{lkq}(r_1 r_2)$ and $\Lambda^{lkq}(r_1 r_2)$ defined by (5) and (6) we can express the pairing field in the form

$$\Delta^{(a)}(r_1 r_2) = \sum_k (-)^k \{[V_{k0}^{qq}(r_1 r_2) - 3V_{k1}^{qq}(r_1 r_2)]/2\} \Theta^{lkq}(r_1 r_2) + \langle lj | \bar{l}\bar{s} | lj \rangle \sum_k (-)^k [V_{k0}^{qq}(r_1 r_2) + V_{k1}^{qq}(r_1 r_2)] \Lambda^{lkq}(r_1 r_2) .$$

In this expression the first and the second term represent the contribution of the singlet even and the

triplet odd components of the interaction, respectively. For reasonable interactions the latter is much weaker than the first one and consequently the singlet-even component will play the dominant role in the determination of the pairing properties of the interaction. Let us mention here that all these expressions apply also to the Coulomb interaction. Finally, what we need in constructing the Bogolyubov Hamiltonian are the matrix elements $\Gamma^{(a)}_{nn'}$ and $\Delta^{(a)}_{nn'}$ which are given by the following integrals:

$$\Gamma^{(a)}_{nn'} = \int \varphi_{ni}(r_1)\Gamma^{(a)}(r_1 r_2)\,\varphi_{n'i}(r_2) r_1^2 r_2^2 dr_1 dr_2$$

and *idem* for $\Delta^{(a)}_{nn'}$. According to the previous definitions they are combinations of the Slater integrals. Their calculation is greatly facilitated by the method we proposed a few years ago.[22]

Concerning the contributions of the DD part of our interaction as well as the two-body spin orbit part, they are easily derived since we choose them to be of zero range. The HF field takes the form

$$\Gamma^q(r_1) = t_0\{(1+\tfrac{1}{2}x_0)\rho^{\alpha+1} - (x_0+\tfrac{1}{2})\rho^\alpha\rho^q + \tfrac{1}{4}\alpha(1-x_0)[\rho^{\alpha+1} + \rho^{\alpha-1}(\kappa^{p2}+\kappa^{n2})] + \alpha(x_0+\tfrac{1}{2})\rho^{\alpha-1}\rho^p\rho^n\}$$
$$+ W_{LS}\left[\frac{1}{r}\frac{d}{dr}(\rho+\rho^q)\overline{ls} - \left(\frac{1}{r}+\frac{d}{dr}\right)(J+J^q)\right],$$

where J^q is the spin density

$$J^q = \frac{2}{4\pi}\sum_b \hat{j}_b^2 \langle j_b \| \overline{ls} \| j_b\rangle \varphi_{n_b l_b}\varphi_{n_d l_b}\rho^{(b)q}_{n_d n_b}$$

and κ^q is what we call the pairing density

$$\kappa^q = \frac{1}{4\pi}\sum (-)^{l_b}\hat{j}_b^2 \varphi_{n_b l_b}\varphi_{n_d l_b}\kappa^{(b)}_{n_d n_b}.$$

For the pairing field the expression is

$$\Delta^{(a)} = t_0\tfrac{1}{2}(1-x_0)(-)^l\rho^\alpha\kappa^q$$
$$+ W_{LS}\frac{\overline{ls}}{r^2}(-)^l\tau^q \quad (a)\equiv(l,j,q),$$

where τ^q, which we shall call the pairing spin density is defined by the equation

$$\tau^q = \frac{1}{4\pi}\sum \hat{j}_b^2 \langle j_b | \overline{ls} | j_b\rangle (-)^{l_b}\varphi_{n_b l_b}\varphi_{n_d l_b}\kappa^{(b)}_{n_d n_b}.$$

Concluding this section, let us add that we also account for the notation of the center of mass by subtracting the usual term $P^2/2mA$ which we treat exactly (direct and exchange terms). Exchange Coulomb term is also treated exactly.

D. Connection of the HFB theory with experimental data

A precise quantitative information of the pairing correlations is not easy to extract in the nuclei. There are no simple physical processes allowing one to isolate completely the pairing effects from the rest. In fact, for most of them we cannot ignore in general the effects associated with the rearrangement (static or dynamic) of the HF average field. In view of this difficulty we describe in this section how we have checked the pairing properties of the effective interaction.

The most direct way of getting information about the pairing is to compare the properties of the odd-even nuclei. Referring to Sugawara,[23] one defines a QP state vector on the HFB vacuum $\eta^\dagger_{i\gamma}|\tilde{0}\rangle$ and minimizes the total energy with this new trial function. The extension of the HFB theory is straightforward since the only modification is in the definition of the generalized density matrix. Thus in all the definitions of Sec. II A we just have to redefine the density matrix and the pairing tensor as

$$\rho_{\alpha\beta} = \langle\tilde{0}|\eta_{i\gamma}a^\dagger_\beta a_\alpha \eta^\dagger_{i\gamma}|\tilde{0}\rangle$$
$$= \langle\tilde{0}|a^\dagger_\beta a_\alpha|\tilde{0}\rangle + \langle\tilde{0}|[\eta_{i\gamma}, a^\dagger_\beta a_\alpha]\eta^\dagger_{i\gamma}|\tilde{0}\rangle,$$
$$\kappa_{\alpha\beta} = \langle\tilde{0}|\eta_{i\gamma}a_\alpha a_\beta \eta^\dagger_{i\gamma}|\tilde{0}\rangle$$
$$= \langle\tilde{0}|a_\alpha a_\beta|\tilde{0}\rangle + \langle\tilde{0}|[\eta_{i\gamma}, a^\dagger_\alpha a_\beta]\eta^\dagger_{i\gamma}|\tilde{0}\rangle,$$

and the minimization leads to the same Bogolyubov condition $[\mathcal{H}, R]=0$. This is the version of the BCS theory of the blocking adapted to the HFB case. Here since we want to maintain the spherical symmetry we take some average by blocking all degenerate QP orbitals inside the same $j\gamma$. This approximation consists in defining the average density matrix in the form

$$\frac{1}{\hat{j}_\gamma^2}\sum_{m\gamma}\langle\tilde{0}|\eta_{i\gamma}a^\dagger_\beta a_\alpha\eta^\dagger_{i\gamma}|\tilde{0}\rangle.$$

Hence we get the following expressions for the density matrix and the pairing tensor:

$$\rho^{(a)}_{nn'} = (V^\dagger V)^{(a)}_{nn'} + \frac{t}{\hat{j}^2}(u^{(a)}_{in}u^{(a)}_{in'} - v^{(a)}_{in}v^{(a)}_{in'})$$
$$\times \delta_{q_\gamma q_\alpha}\delta_{l_\gamma l_\alpha}\delta_{j_\gamma j_\alpha} \quad (a)\equiv(l_\alpha, j_\alpha, q_\alpha),$$
$$\kappa^{(a)}_{nn'} = (U^\dagger V)^{(a)}_{nn'} - \frac{1}{\hat{j}^2}(u^{(a)}_{in}v^{(a)}_{in} + u^{(a)}_{in}v^{(a)}_{in'})$$
$$\times \delta_{q_\gamma q_\alpha}\delta_{l_\gamma l_\alpha}\delta_{j_\gamma j_\alpha}.$$

It is obvious that the Bogolyubov conditions depend now on the "blocked" QP state $i\gamma$. The blocked state which leads to the lowest total

energy will be associated with the ground state of the odd nucleus in question. The other QP states may serve to describe the low lying excited states. In this way we have calculated the odd-even mass difference discussed below and the first excited levels of some odd nuclei. As pointed out by other authors,[24] there is an important difference between the problems with even and odd particle number. In the odd case the Bogolyubov conditions only imply that the ground state and the 3QP states $\eta^\dagger_{k\alpha}\eta^\dagger_{l\beta}\eta^\dagger_{i\gamma}|\tilde{0}\rangle$ are not coupled in first order perturbation. All other 3QP states not containing the blocked QP, $\eta^\dagger_{i\gamma}$ can be coupled to the ground state by the residual interaction. Thus one should include them in the description of the odd system. It could be done by coupling the added QP with the core excitations of the even nucleus (QP phonon coupling). However, we limited ourselves to the HFB theory and we have just emphasized this question for the discussion presented below. Finally, another check of these calculations is provided by the stripping and pickup reactions which can be related to the occupation probabilities.

E. Numerical method of solving HFB equations

The HFB equations are solved by an iterative procedure. To initiate the iteration we guess a density matrix $\rho^{(0)}$ and a pairing tensor $\kappa^{(0)}$ in order to calculate the Bogolyubov Hamiltonian $\mathcal{H}^{(0)}$. The diagonalization of $\mathcal{H}^{(0)}$ provides a set of QP states which permits us to calculate a new set $\rho^{(1)}$ and $\kappa^{(1)}$ according to the expressions given in Sec. II B. With this new set we calculate $\mathcal{H}^{(1)}$ and diagonalize it, etc. We stop the iterations when the differences $\max(\rho^{(I)}_{\alpha\beta}-\rho^{(I+1)}_{\alpha\beta})$ and $\max(\kappa^{(I)}_{\alpha\beta}-\kappa^{(I+1)}_{\alpha\beta})$ are less than some prescribed value ϵ. For all calculations reported here we chose $\epsilon\simeq 10^{-4}$. Concerning the starting $\rho^{(0)}$ and $\kappa^{(0)}$, we first perform a HF calculation without necessarily achieving an accurate convergency, and on the corresponding HF basis we guess some occupation probabilities around the Fermi surface needed to define the pairing tensor $\kappa^{(0)}$. We also mention that at the beginning of the iteration procedure we must slow down the convergence on the density matrix by making some weighting between two successive iterations. In this way the average field varies slowly and we can insure the convergence on the pairing tensor step by step. Furthermore, we readjust the mean number of protons and neutrons at each HFB iteration by the following perturbation method.

For the discussion let us suppose that at some iteration, say I, the HFB Hamiltonian $\mathcal{H}^{(I)}(\lambda)$ provides a set of QP states such that $\langle\hat{N}\rangle=N$ instead of the prescribed value N_0. The problem is to readjust the Lagrange parameter λ so as to get the correct answer $\mathrm{tr}\rho=N_0$. To this end we determine the variation of the generalized density matrix induced by a variation $\delta\lambda$ in the equation $[\mathcal{H}(\lambda+\delta\lambda),R(\lambda+\delta\lambda)]=0$. We set $R(\lambda+\delta\lambda)=R(\lambda)+\delta\lambda^{(1)}R$ with the condition $[\mathcal{H}(\lambda),R(\lambda)]=0$. Neglecting the rearrangement of $\mathcal{H}$ we get at first order in the basis diagonalizing $R(\lambda)$,

$$^{(1)}R^{pq}_{ik}=\delta\lambda\frac{N^{pq}_{ik}}{\epsilon_i+\epsilon_k},\quad p,q=1,2\,.$$

We refer to Appendix C for the notations. Thus we can express $\delta\lambda$ in terms of $\Delta=N_0-N=\frac{1}{2}\mathrm{tr}\hat{N}^{(1)}R$. In our case we have two separate corrections for the neutrons and the protons. Their expressions are

$$\delta\lambda^q=\Delta/4\sum_{k\neq i}\hat{j}^2[UV]_{ik}{}^2/(\epsilon_i+\epsilon_k)\,.$$

Then with these two corrected Lagrange parameters we diagonalize $\mathcal{H}(\lambda+\delta\lambda)$ and check the mean number of particles. If the perturbation method was legitimate we get the correct answer $N=N_0$. If not, we repeat the process starting from $\mathcal{H}(\lambda+\delta\lambda)$ until it converges. In fact, at the first few HFB iterations we need two or three nested iterations, but rapidly after three or four HFB iterations the procedure described above gives the good correction right away. Evidently we can apply this method to any type of constraint. Finally, let us mention that we are able to include 15 shells of harmonic oscillator in our basis $[2(n-1)+l\leq 14]$. We give computational time for different size of the basis in Table I. On account of the amount of work necessary in such calculations, one can realize the great efficiency of our methods and also of the codes.

TABLE I. Computing time for one HF or HFB iteration as a function of the dimensions of the basis (N_0).

OH basis N_0		8	10	12	14
Time (sec) on IBM 36091 of Saclay	HF	1	1.5	2.5	5
	HFB	1.5	3	5	10

III. THE DENSITY-DEPENDENT EFFECTIVE INTERACTION

The derivation of our effective interaction was done essentially along the line described by Brink and Boeker.[25] Such derivation is purely phenomenological in the sense that the interaction has a predetermined form whose parameters are adjusted to reproduce the global properties of the nuclei and the empirical data in nuclear

matter. It is in that spirit that the Skyrme interactions and some others were derived. In this section we devote a part to the concise description of the criteria we used to achieve the fit. A second part concerns the nuclear matter. There we exhibit the properties and the global behavior of an interaction we selected with such a fit. Finally, the important role of a finite range in the force is discussed in the last part. In order to avoid the misunderstandings we call a zero range force all forces obtained by the δ-force parametrization and by finite range force are meant the forces parametrized by analytical functions (such as Gaussian, Yukawa, etc.).

A. Description of the effective interaction

We have postulated an interaction of the form

$$V(\mathbf{r}) = \sum_{i=1,2} (W + BP_\sigma - HP_\tau - MP_\sigma P_\tau)_i \, e^{-r^2/\mu_i^2}$$
$$+ t_0(1 + x_0 P_\sigma)\rho^\alpha\left(\frac{\mathbf{r}_1 + \mathbf{r}_2}{2}\right)\delta(\mathbf{r}_1 - \mathbf{r}_2)$$
$$+ iW_{LS}(\sigma_1 + \sigma_2)\overleftarrow{\nabla}_1 - \overleftarrow{\nabla}_2 \delta(\mathbf{r}_1 - \mathbf{r}_2)\overrightarrow{\nabla}_1 - \overrightarrow{\nabla}_2 ,$$

i.e., the sum of central and spin orbit terms. For the latter we have retained the form given by Skyrme. Its intensity was fitted independently of the other parameters so as to reproduce the splitting $(p^{3/2} - p^{1/2})$ in ^{16}O.

The central force separates into two parts. One is independent of the density and is inspired by the works of Volkov[26] and Brink and Boeker. It is composed of two Gaussians, one of which simulates a short range and the other one an intermediate range. Furthermore, it contains all possible admixtures of spin, isospin, and space exchange operators denoted, respectively, as P_σ, P_τ, P_x. We took Gaussian shapes because of their computational advantages when extending the calculations to the case of deformed nuclei. The other part is density dependent and is chosen of zero range in order to reduce computation time to a minimum. Although this form—acting only in the even states—is probably too simplified, we shall see in the section concerning the nuclear matter that it still allows us to reproduce closely enough the mechanism of saturation obtained with the fundamental approach based on the Brueckner theory. Concerning the adjustment of the parameters, we start with a given set $(t_0, x_0, \alpha, \mu_1, \mu_2)$ and we determine linear equations in the other parameters so as to get the global properties of some spherical nuclei. These equations being extracted with the restricted HF procedure we must allow for the variation of the results when passing from the restricted to the complete HFB calculation.

We shall not enter into the details of the fitting procedure. We only indicate that we adjust the saturation properties of the ^{16}O and ^{90}Zr combined with some of the empirical data in nuclear matter (symmetry energy, for instance). Furthermore, since we also want to determine the pairing properties of the force we include equations associated to the matrix elements of the form $\langle (nS)^2 0T = 1 | V | (nS)^2 0T = 1 \rangle$ $(nS) = (1S)$, $(2S)$, i.e., those which depend on the singlet-even component of the force. As for these matrix elements, their values are not precisely determined and we only know that they must be negative in order to get pairing correlations. Thus we consider them as free parameters in the fit. Owing to the fact they can be varied without destroying the properties depending on HF alone, we have been able to find an interaction giving not only a good description of the average field but also providing a fair description of pairing effects where they sensibly affect the calculations. From now on we shall

TABLE II. The coefficients needed in the definition of E^{ST} (see the text) which represent the potential energy in nuclear matter for each subspace ST.

ST	00	01	10	11
$4\sqrt{\pi}\,A_i^{(ST)}$	$(W+H-B-M)_i$	$3(W+M-B-H)_i$	$3(W+M+B+H)_i$	$9(W+B-H-M)_i$
$B_i^{(ST)}$	A_i^{00}	$-A_i^{01}$	$-A_i^{10}$	A_i^{11}
$C^{(ST)}$	0	$\frac{(1-x_0)}{2}\frac{3t_0}{8}$	$\frac{(1+x_0)}{2}\frac{3t_0}{8}$	0

The values of the parameters for $D1$ and $D1'$

Range fm	W	B	H	M MeV	α	to MeV fm^4	x_0
0.7	−402.4	−100.0	−496.2	−23.56	$\frac{1}{3}$	1350	1
1.2	−21.30	−11.77	37.27	−68.81			

$W_{LS} = 115$ for $D1$ $\quad$ $W_{LS} = 130$ for $D1'$

TABLE III. The nuclear matter properties calculated with the $D1$ force. $-E/A$ binding energy per particle. $-k_F$ Fermi momentum. $-K$ Incompressibility. $-a_s$ volume symmetry coefficient. $-m^*/m$ Effective mass.

	E/A	k_F (fm^{-1})	K (MeV)	a_s (MeV)	m^*/m
$D1$	16.32	1.35	228.0	30.8	0.67

denote this effective interaction as $D1$. (See Table II for its definition.) As stated below, we also use an interaction $D1'$ which differs from $D1$ in the value of spin orbit coefficient.

B. Properties of $D1$ in nuclear matter

In order to present a complete survey of the proper behavior of $D1$, we have considered it useful to report in some detail the calculations in the nuclear matter.

The quantities discussed in the following are extracted from the formula (3). This expression is very useful since it determines not only the saturation properties of the force but it provides also very interesting information on the force when departing slightly from the equilibrium via all possible particle-hole excitations. Thus we specialize this expression to the case of the nuclear matter, i.e., we use plane wave functions including spin and isospin $[(1/\sqrt{\Omega})e^{i\vec{k}\vec{r}}\chi_m^{1/2}\chi_q^{1/2}]$ and furthermore we neglect the pairing.

We have decomposed the total binding energy $E(\rho^{(0)})$ into the different contributions $E^{(ST)}$ of the potential energy in each subspace (ST) defined by the projectors $P^{(ST)}=(1\pm P_\sigma)(1\pm P_\tau)/4$. Consequently, the total energy per particle is written as $E/A=T/A+\sum_{ST}E^{(ST)}/A$, where T represents the kinetic energy and $E^{(ST)}$ the potential energy whose expression is given by

$$E^{ST}=\sum_{i=1,2}A_i^{(ST)}X_i^3-B_i^{(ST)}\left[\left(\frac{1}{2X_i}-\frac{1}{X_i^3}\right)e^{-X_i^2}-\frac{3}{2X_i}+\frac{1}{X_i^3}+\frac{\sqrt{\pi}}{2}\operatorname{erf}(X_i)\right]+C^{(ST)}\rho^{\alpha+1}(k_F).$$

The coefficients $A_i^{(ST)}$, $B_i^{(ST)}$, C^{ST} and the definition of X_i are given in Table II and $\rho(k_F)=2k_F^3/3\pi^2$. The error function is defined according to $\operatorname{erf}(X)=2/\sqrt{\pi}\int_0^X\exp(-t^2)dt$. The density of saturation is given by the k_F which minimizes the energy. We report in Table III the k_F and the corresponding E/A calculated with $D1$.

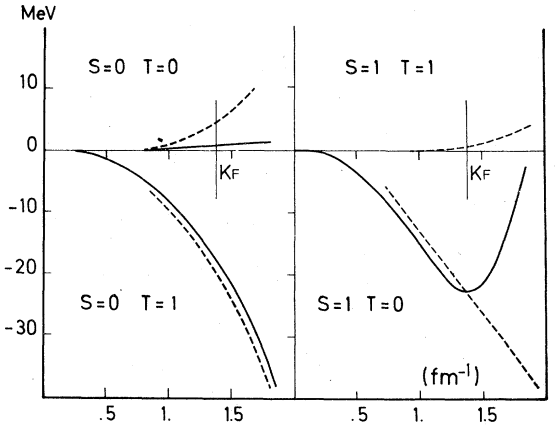

FIG. 1. The contributions to the nuclear matter potential energy corresponding to the different components $^{(ST)}V$ of the effective force. The dashed lines represent the general trend of the ones obtained with more fundamental nuclear matter calculations using realistic two-body interactions and the Brueckner HF theory.

The decomposition of E/A according to the different contributions $E^{(ST)}$ was performed in order to exhibit the mechanism of the saturation. In Fig. 1 we recognize that most of the contribution to the nuclear matter potential energy comes from the even parts $E^{(01)}$, $E^{(10)}$, at least for the momenta from zero up to 1.65 fm^{-1}. We also notice that the triplet-even potential energy plays an important role in the mechanism of saturation; a result which is quite similar to what happens in the nuclear matter calculations using G matrix.[27] More generally, the fact that we reproduce the trend of the saturation curves obtained with more fundamental approach is an indication that $D1$, although phenomenological, is a reasonable parametrization of a G matrix corrected to give the correct saturation properties (cf. Ref. 1). However, it is clear that this parametrization does not account for the energy dependence of a G matrix and that a finite range in the dependence on the density would be more realistic in describing the momenta below 1.7 fm^{-1}.

Now we come back to the second order variation of the energy in the formula (3). Using the notation $\rho^{ST}_{k+q,k}$, where $\vec{q}$ is the momentum transfer between a particle and a hole and S and T represent the total spin and isospin of a particle-hole pair, we get the following expression for the second order energy $^{(2)}E$:

$$\sum_{q^{ST}}\sum_{\substack{|k'|<k_F\\ |k'+q|,\ |k+q|>k_F}}\sum_{|k|<k_F}|\rho^{ST}_{k+q,k}\rho^{ST*}_{k-q,k}|\begin{pmatrix}A^{ST}_{k+q,k;k'+q,k'} & B^{ST}_{k+q,k;k'-q,k'}\\ B^{ST}_{k-q,k;k'-q,k'} & A^{ST}_{k-q,k;k'-q,k'}\end{pmatrix}\begin{pmatrix}\rho^{ST*}_{k'+q,k'}\\ \rho^{ST}_{k'-q,k'}\end{pmatrix},$$

where A^{ST} and B^{ST} are related to the second derivation of the total energy with respect to the density matrix.

It is interesting to calculate the contribution associated to the small momentum transfer $q \ll 1$. In that case, at first order in q the summation over $|\vec{k}|$ becomes $\pm[\Omega/(2\pi^3)]q^2 k_F{}^2 \cos\theta$ with $\theta = (\hat{kq})$, so that the particle-hole pairs are on the Fermi surface. As a consequence, we need only to consider the set of variable $\hat{X} = (\theta, \varphi)$ characterizing the direction of $\vec{k}$ with respect to $\vec{q}$. Thus, setting

$$\Phi(\hat{X}) = \cos\theta \rho^{ST}_{k_F}(\hat{X}) \quad \cos\theta > 0$$

and

$$\Phi(\hat{X}) = -\cos\theta \rho^{ST}_{k_F}(\hat{X}), \quad \cos\theta < 0$$

the second order energy ${}^{(2)}E$ becomes

$${}^{(2)}E_q = \frac{4\pi}{N\Omega}\left[\frac{\Omega}{(2\pi)^3}\right]^2 (qk^2)^2 \times \iint d\hat{X}\, d\hat{X}' \left[\delta(X - X') + \frac{N}{4\pi} V^{ST}(X, X')\right] \times \Phi^{ST}(X)\Phi^{ST}(X')^*,$$

where $N = mk_F/h^2 2\pi^2$ is the density of states at the Fermi surface and m is the effective mass. Furthermore, we get this simple form because in the limit $q \to 0$ the particle-hole matrix elements entering in the definition of A^{ST} and B^{ST} are identical.

Introducing the multipole decomposition $V^{ST}(\hat{X}, \hat{X}') = \sum_l V_l \; P_l(X, X')$ and $\Phi(\hat{x}) = \sum \Phi_{lm} P_{lm}(\hat{x})$, we express easily the stability condition $({}^{(2)}E > 0)$ with respect to all possible particle-hole excitations associated with the various deformations of the Fermi surface in the different channels S, T. We find $1 + F_l^{ST}/(2l+1) > 0$ where $F_l^{ST} = NV_l^{ST}$. These are the conditions on the multipole of the particle-hole interaction which warrants that the HF solution is a local minimum. At this stage it is worthwhile to point out that the quantization of ${}^{(2)}E_q$ would lead to a transport equation [it is the limit of the random phase approximation (RPA) equation as $q \to 0$] which permits us to interpret the F_l as the Landau parameters associated to our effective interaction. Thus all the formulas of the Fermi liquid theory which express the effective mass, the incompressibility, and the symmetry energy in terms of the F_l may be transposed to our case. Their expression reads

$$\frac{m^*}{m} = (1 + \tfrac{1}{3}F_1^{00}),$$

$$K = \frac{3\hbar^2 k_F{}^2}{m^*}(1 + F_0^{00}),$$

$$a_s = \frac{\hbar^2 k_F{}^2}{6m^*}(1 + F_0^{01}),$$

and their values calculated with $D1$ are listed in Table III. We do not list here the Landau parameters associated to the interaction $D1$ since they are given elsewhere (see Ref. 21). We just mention that all the stability conditions are satisfied by the particle-hole interaction extracted from $D1$. Furthermore, let us add that a study[28] of the monopole resonances in the finite nuclei supports the value of the nuclear matter incompressibility obtained with $D1$.

Finally, in order to complete the review of the properties of $D1$ in the nuclear matter we refer the reader to the following articles; one[21] concerns the propagation of the collective modes. It is shown that the Landau parameters of $D1$ reproduce well some previous microscopic calculations with Reid soft core potential G matrix. The other[29] is complete HF calculation on semi-infinite nuclear matter with $D1$. There the value $a_{sf} = 20.1$ MeV is extracted for the surface coefficient of the mass formula very close to the values proposed by Myers (20.69) and Groote Hill and Takahashi (20.85).

C. Why the finite range?

In order to explain the motivations which led us to introduce a finite range in the course of construction of $D1$, we discuss some aspects which are related to the choice of the zero range effective interactions. Of course it is not our intention to discredit the excellent results obtained with the zero range effective interactions but rather to indicate the limitations in their applications.

If we believe that the effective force is something like a G matrix, the presence of finite range leaves no doubt and the first question is to understand its influence on the HF results. The density matrix expansion (DME) derived by Negele and Vautherin[30] is the convenient tool to study the role of the finite range. These authors have shown on the proton distribution the effect of truncating their expansion to the few terms corresponding to a Skyrme's force. They conclude that the exact DDHF and such DME calculations lead to shell model fluctuations which are significantly different.

It is a consequence of the fact that the long range of the force smoothes the fluctuations of the HF field as compared to a short range interaction which takes into account the local variation in the HF density; an effect which is emphasized by the self-consistency. For the same reason one may wonder if the short range forces can

always simulate the long range or the intermediate range when studying the response of the nuclei to an external field as one does for instance to get the potential energy surfaces as function of deformation. Clearly this question is important if we try to understand the limitations of the HF theory itself.

The role of the finite range is still more crucial when one desires to extend the theory beyond the HF approximation. In reality the fact that pathologies may exist when putting the range of the interaction to zero is clearly seen when analyzing the Fourier transform of the zero range forces. In particular, one recognizes that their behavior with high relative momenta is completely unrealistic. For example, these forces contain terms constant or increasing quadratically in the relative momenta instead of vanishing rapidly as it is the case in the calculations with finite range forces. Such unrealistic feature is not too dramatic in the HF calculation because one only needs the low Fourier components in the relative momenta which never exceed $2k_F$, but as soon as one wants to go beyond HF the situation is quite different. Thus, in the case which interests us directly, i.e., in the HFB procedure, the particle-particle matrix elements enter in the calculations and in principle there is no restriction on the Fourier components interfering in this procedure. The difficulty we discuss here is well illustrated in the BCS approach to the pairing with a constant pairing force. As is well known, the corresponding gap equations must be solved in a restricted space, otherwise these equations would be divergent in the whole space. That is to say, the smearing of the Fermi surface due to the pairing is restricted arbitrarily over particle states close to the Fermi surface. In such an approach to the pairing it has been recognized that there is a crucial interdependence between the pairing force intensity and the one particle level density. We agree that it may be a reasonable way to take into account the essential features of pairing effects in some specific studies but we believe that the proper pairing theory constructed for the systematic use does not tolerate such *ad hoc* procedures. Clearly the finite range force allows us to avoid such *ad hoc* truncations since they will automatically result from the properties of the interaction itself. In our view this is the only way to define an approach to the pairing which is completely self-consistent and general enough. Finally, although we are not directly concerned here with the RPA calculations, let us mention another pathology when employing zero range force, namely that we get too much collectivity for the states at high energy. This is easily understood by analyzing the RPA particle-hole Green's function which never tends to the free particle-hole Green's function as it should as the transfer $q \to \infty$. It is a consequence of the unrealistic behavior of particle-hole interaction at the high momentum transfer.

IV. HFB CALCULATIONS OF THE FINITE SPHERICAL NUCLEI

In this chapter we collect together a large set of various results on the static properties of the spherical nuclei extracted with the HFB procedure using the effective interaction $D1$. We clarify that we do not only present the results for the superfluid nuclei but also for the normal ones, which would be satisfactorily described by the HF approximation alone. We never mention the HF procedure because it is automatically included in the HFB approximation. Nevertheless, our primary aim being to demonstrate that we have a reasonable approach to the pairing, we devote the first section to the presentation of the results which concern directly the pairing effects.

A. Results associated with the pairing effects

This section is mostly devoted to the study of the isotopes of the tin nuclei. We have chosen those isotopes for several reasons. First of all, they are spherical nuclei which can be treated in good approximation in the framework of the independent QP model. Second, there is a wide range of isotopes which permit us to follow the features of this approach and in particular to check how it reproduces the variation of the pairing as function of the neutron number. Finally, there are numerous experimental data as well as many theoretical works on this series of isotopes providing us with useful informations.

We first discuss briefly the accuracy of the HFB calculations. In the definition (4) we restrict the summation on the radial quantum number n according to the relation $0 \leq 2(n-1)+l \leq N_0$, where N_0 denotes the number of oscillator quanta. The calculations on the tin isotopes are performed with $N_0 = 10$ and those on lead with $N_0 = 12$. The oscillator length $b = (\hbar/m\omega)^{1/2}$ we use in HFB is determined by minimizing the HF energy. Furthermore, it was checked on ^{116,117,118,124,132}Sn and ^{208}Pb that all the quantities studied here did not change significantly when passing from $N_0 = 10$ to 12 for tin isotopes and from $N_0 = 12$ to 14 for ^{208}Pb. For example, the increase of binding energy for tin isotopes is about 2 MeV (see Table IV) and 1.6 MeV for ^{208}Pb.

We investigate all the even-even and odd-even

TABLE IV. Comparison between some calculations including $N_0=12$ harmonic oscillator shells in the basis, and $N_0=10$ calculations. See Table V.

Sn	$-E_{\mathrm{HFB}}$	Δ_{HFB}	$-E_p$	$-(E_{\mathrm{HFB}_{12}}-E_{\mathrm{HFB}_{10}})$
116	990.455		18.81	1.516
117	997.412	1.385	14.87	1.552
118	1007.138		18.87	1.585
124	1052.640		17.24	2.062
132	1104.926		0	2.226

tin isotopes whose mass number cover the range $112<A<125$. We comment first on Table V where we have listed the total binding energies of these nuclei. In order to show the pairing effects we give separately the two contributions occuring in the definition of the HFB energy. One has the form of the usual HF energy,

$$E^{B}_{\mathrm{HF}}(\rho^0,\kappa^0)=\mathrm{tr}[T+\tfrac{1}{2}\Gamma(\rho^0,\kappa^0)]\rho^0 .$$

We use the notation E^{B}_{HF} to avoid eventual confusion. In fact, this contribution is evaluated with the density matrix extracted from a complete HFB calculation and generally differs from the one obtained with the density extracted from a HF calculation. In particular, denoting by E_{HF} the contribution in the latter case, we know that E^{B}_{HF} satisfies the relation $E^{B}_{\mathrm{HF}}\geq E_{\mathrm{HF}}$ since by definition E_{HF} is minimum (they are equal for vanishing pairing correlations). The other contribution is just given by $E_p=\frac{1}{2}\mathrm{tr}\Delta\kappa$ which provides us with a measure of the importance of the pairing correlations. Thus the HFB binding energy is written as $E_{\mathrm{HF}}=E^{B}_{\mathrm{HF}}+E_p$. From Table V we conclude that the tin isotopes in the range $112\leq A\leq 124$ are superfluid since, for all of them, we find a non-negligible pairing energy of the order of 16 MeV. As expected, only the neutrons contribute to E_p since the proton pairing correlations vanish due to the shell closure at the proton number $Z=50$. In connection with the previous discussion on the definition of E^{B}_{HF} we mention that these 16 MeV do not represent the gain of binding energy as compared to the HF binding energy of the HF procedure alone. In reality E^{B}_{HF} decreases rapidly with an increasing diffuseness at the Fermi surface and it is the competition between the loss energy on E^{B}_{HF} and the gain energy on E_p which determines the trend toward a superfluid solution. As a matter of fact, the contribution E^{B}_{HF} decreases quickly with the diffuseness of the Fermi sea so that E_{HFB} and E_{HF} differ in general by only a few MeV (see Table V, last column). We emphasize that it does not mean that the pairing is a small effect, since obviously the quantity E_p indicates a significant difference between the HF and HFB wave functions.

In order to stress the difference between the wave functions, we have drawn in Fig. 2 the neutron density calculated with both procedures in the case of ^{116}Sn. We note the great difference between the two predictions from the center up to a radius of about 3 fm. In contrast the two neutron distributions are the same at the surface.

TABLE V. The results of the HFB calculations with $D1$ in the tin isotopes. This calculation included $N_0=10$ shells of harmonic oscillator. The two-body part of the center of mass motion (C.M. correction) has been omitted. E_{HFB}, E^{P}, and E^{B}_{HF} represent, respectively the total HFB energy, the total pairing correlation energy, and $E^{B}_{\mathrm{HF}}=E_{\mathrm{HFB}}-E^{P}$. $J^{\pi}_{\mathrm{g.s.}}$ is the parity and the spin of the ground state, and Δ denotes the odd-even mass differences. We recall that in the Fig. 9, extrapolation to infinite HO basis and C.M. correction have been taken into account.

Sn	B_{exp}	Δ_{exp}	$J^{\pi}_{\mathrm{g.s.\ exp}}$	$-E_{\mathrm{HFB}}$	Δ_{HFB}	$J^{\pi}_{\mathrm{g.s.\ HFB}}$	$-E^{B}_{\mathrm{HF}}$	$-E_p$	$-E_{\mathrm{HF}}$	$-(E_{\mathrm{HFB}}-E_{\mathrm{HF}})$
112	953.538			953.065			934.79	18.27	948.301	4.764
113	961.284	1.271	$\frac{1}{2}^+$	960.641	1.609	$\frac{1}{2}^+$		14.85		
114	971.583			971.434			953.80	17.63	968.403	3.031
115	979.130	1.007	$\frac{1}{2}^+$	978.585	1.402	$\frac{1}{2}^+$		13.52		
116	988.692			988.939			972.01	16.93	985.701	3.238
117	995.636	1.192	$\frac{1}{2}^+$	995.860	1.386	$\frac{1}{2}^+$		12.82		
118	1004.963			1005.553			989.00	16.55	1002.164	3.389
119	1011.447	1.311	$\frac{1}{2}^+$	1011.891	1.541	$\frac{1}{2}^+$		12.96		
120	1020.554			1021.310			1004.94	16.37	1018.898	2.412
121	1026.725	1.322	$\frac{3}{2}^+$	1027.136	1.667	$\frac{11}{2}^-$		12.46		
122	1035.541			1036.295			1020 16	16.14	1032.187	4.108
123	1041.487	1.272	$\frac{11}{2}^-$	1041.988	1.462	$\frac{11}{2}^-$		12.06		
124	1049.978			1050.605			1035.20	15.40	1045.901	4.704
125	1055.711		$\frac{11}{2}^-$	1056.121		$\frac{11}{2}^-$		11.05		
132	1102.700			1102.772			1102.77	0	1102.772	0

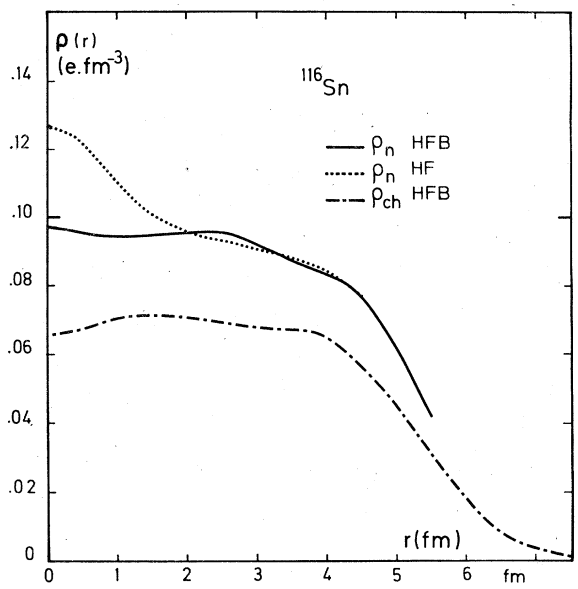

FIG. 2. This figure exhibits the influence of pairing correlations on the neutron density distribution of ^{116}Sn.

All this is easily understood in terms of the spectroscopic factor given below. Let us also mention that the proton density is distorted indirectly, via the pairing between the neutrons but this effect is much smaller (see Fig. 2).

The odd-even mass differences make part of the basic quantities considered in all the studies concerning the pairing. The reason is that they represent somehow the energy needed to break a pair when picturing the pair as two particles interacting in two time reversed orbitals. Thus these data are considered as providing a direct information on the pairing correlations in the nuclei. On the other hand, under certain assumptions these data have a simple connection with the theory. In fact, describing the odd nucleus as the one QP state $\eta^{+}_{i\nu}|\tilde{0}\rangle$ ($|\tilde{0}\rangle$ is the ground state of the neighboring even nucleus) and neglecting all rearrangement effects when passing from one nucleus to another, we recall the well known relation between the odd-even mass difference and the lowest QP energy:

$$\epsilon = -[B(A) - 2B(A-1) + B(A-2)]/2\,, \quad A \text{ even}\,.$$

Although such an approximation has the merit of giving a simple check on the theory by requiring only the calculation of the even nuclei, it presents also the disadvantage of providing too rough a comparison with the experiment. Besides, in our case, this relation needs to be corrected by an extra term which accounts for the explicit dependence on the density of the effective interaction we use. Thus we have chosen to calculate the right-hand side of the equation above as follows. We perform separate HFB calculations of the binding energies of the three adjacent nuclei. Concerning the odd nuclei we use the blocking version of the HFB theory described in Sec. II. We point out that we do perform complete HFB by blocking the few lowest QP since we do not know *a priori* which one corresponds to the ground state. In that way we determine not only the ground state but also the first low lying excited states of the odd nuclei.

In Fig. 3 we have reported the HFB odd-even mass differences along with the experimental values and we also give in Table V for each isotope the spin of its ground state as predicted by the HFB calculations. First we notice that the HFB calculations reproduce the oscillating trends which are observed experimentally as a function of the neutron number. Concerning the magnitude of our predictions, they are all shifted above the experimental value by amount of the order of 300 keV. Somehow such deviation is desirable since one expects that the residual interaction between the three QP states (or the QP vibration coupling) would lower the ground state energy of the odd nuclei which goes in the right sense. Referring to the work of Kuo *et al.*[31] on the odd tin isotopes, we learn that such correction may be of some hundred keV representing the order of magnitude we need precisely to improve the comparison with the experimental data. Of course this argument is purely qualitative and one should evaluate this correction with the QP vibration coupling expressed with our effective interaction in order to draw a definite conclusion. This discussion reveals the inherent difficulty met while adopting the concept of a phenomenological effective interaction. That is,

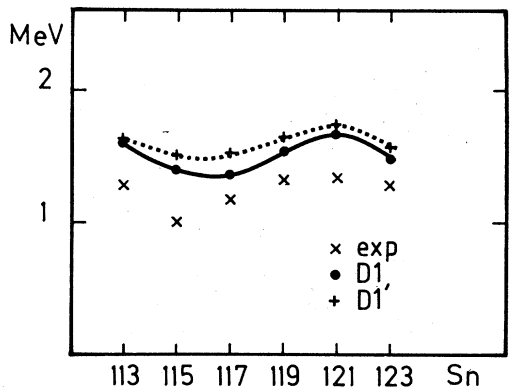

FIG. 3. The odd-even mass differences for the tin isotopes calculated with the two effective interactions $D1$ and $D1'$.

having no precise idea concerning relative importance of the higher-order corrections, we never know the accuracy one should require at a given level of approximation.

Turning back to Table V we notice another encouraging feature of these calculations which except for ^{121}Sn predict the right spin for the ground state of all the tin isotopes investigated here. With respect to the ^{121}Sn, our calculation predicts a $\frac{11}{2}^-$ instead a $\frac{3}{2}^+$ level, but experimentally these levels are separated by only 8 keV and in our calculations by 150 keV. The reasons we have to be satisfied with such predictions are better understood by looking at Fig. 4 where we have reported the experimental situation concerning the first low lying states of the odd tin nuclei. The first two or three states are in general all contained in an energy range of a few hundred keV; consequently, it is remarkable that the use of a microscopic approach permits to extract among them the right spin for the ground states. At this stage it is worthwhile to recall that we use exclusively the effective interaction $D1$ derived as explained in Sec. III. In particular, nothing has been done to adjust the HF average field in that region and also the pairing properties of the interaction associated with the singlet-even component of $D1$ was only adjusted to reproduce at best the odd-even mass differences discussed above.

Although the one QP picture has been found insufficient even for the low lying states, we have thought of some interest to report the lowest excited states calculated with the blocking version of the HFB theory. We give two sets of results, one set corresponds to the interaction $D1$ and the other, named $D1'$ in the following, is calculated by increasing by about 10% the intensity of the two-body spin orbit of $D1$. The $(p_{3/2}-p_{1/2})$ neutrons splitting in ^{16}O is 5.7 MeV with $D1$ ($W_{LS}=115$) and 6.3 MeV with the new intensity ($W_{LS}=130$) to be compared with an experimental value of the order of 6.1 MeV. Let us also mention that initially we did not take into account the two-body contribution of the center of mass to the HF field. Without this contribution one gets $(p_{3/2}-p_{1/2})\simeq 6$ MeV with $W_{LS}=115$. We recognized later that this contribution might reduce significantly the spin orbit splitting in the light nuclei and consequently a W_{LS} of the order of 130 MeV has appeared to be a more appropriate value. However, as we did not want to repeat the lengthy computations performed before, we decided to present all the results with $D1$ ($W_{LS}=115$) and to give also the more recent results with $D1'$ ($W_{LS}=130$), including the two-body contribution of the center of mass. Except for the spin orbit splitting there is not a significant difference between $D1$ and $D1'$.

Turning back to Fig. 4, the HFB spectrum reproduces the essential features of the experiment in particular with $W_{LS}=130$. This result is rather encouraging especially when one remembers that the first attempts[32] to reproduce the spectrum of these isotopes did not do much better despite the seven free parameters used in these works. The same type of discussion applies to Fig. 5 where we give the spectroscopic factors

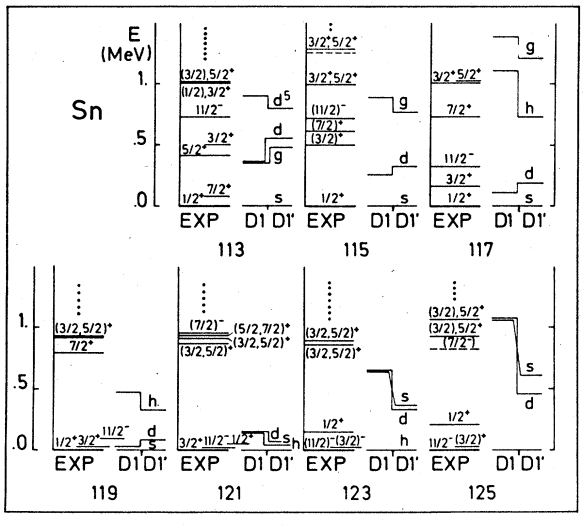

FIG. 4. The first low lying excited states of the odd tin isotopes [*Nuclear Data Sheets* (Academic, New York, 1973)] compared to the one QP spectrum resulting from the blocking version of the HFB theory (see the text). (s,g,d,d^5,h) stands, respectively, for $(s^{1/2},g^{7/2},d^{3/2},d^{5/2},h^{11/2})$.

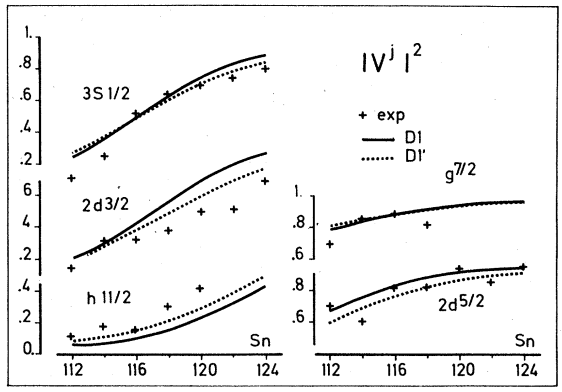

FIG. 5. The HFB spectroscopic factors calculated with the $D1$ and $D1'$ interactions and compared with the experimental values extracted from the (d,t) and (d,p) reactions [E. J. Schneid *et al.*, Phys. Rev. 156, 1316 (1967)].

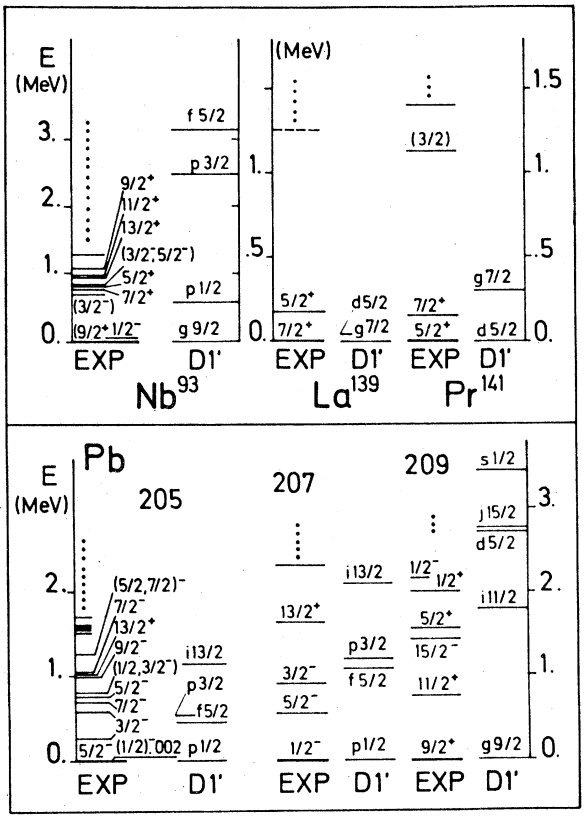

FIG. 6. The first low lying excited states of various odd nuclei compared to the one QP HFB spectrum calculated with $D1'$ (exp., see Fig. 4).

calculated with our QP amplitudes.

Furthermore, in order to show that the nice feature we obtain on the tin isotopes is not fortuitous, we refer to Fig. 6 which contains the results of similar studies on ^{93}Nb, the odd isotopes ($N = 82$) ^{139}La and ^{141}Pr, and the lead isotopes. We see that according to our discussion below, the level sequence of QP spectrum is well reproduced when the first collective state stands at high excitation. This is the case for ^{139}La and ^{141}Pr. For lead isotopes the first collective state (3^-) lies at 2.61 MeV in ^{208}Pb. It is lowered at 0.8 MeV (2^+) in ^{206}Pb. The same is true for $^{93}_{41}$Nb near the $^{92}_{40}$Zr where the first excited state (2^+) lies at 0.93 MeV while the first one (0^+) in $^{90}_{40}$Zr lies at 1.75 MeV.

Finally, in Fig. 7, we report the calculations of the charge densities for two nuclei ^{90}Zr and ^{140}Ce. The ^{140}Ce is of particular interest to us, since it shows the crucial effect of the pairing correlations on the charge density distribution. Besides, this effect is still discernible even in the case of a closed shell nucleus such as ^{90}Zr.

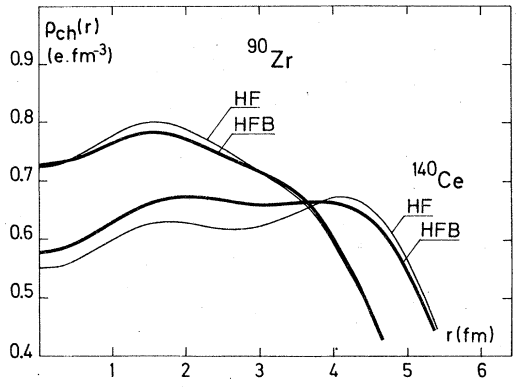

FIG. 7. The influence of pairing correlations on the charge distributions of the semimagic nuclei ^{90}Zr and ^{140}Ce.

V. THE DESCRIPTION OF THE BULK PROPERTIES

The previous section was mainly devoted to the description of the physical quantities related to the fine details as compared to the global properties whose description depends essentially on the characteristics of the average HF field. In order to show the large domain of validity of our self-consistent approach we now present the results concerning the gross properties of nuclei in their ground states. The sample of nuclei investigated cover different regions of the periodic table where the assumption of spherical symmetry looks reasonable.

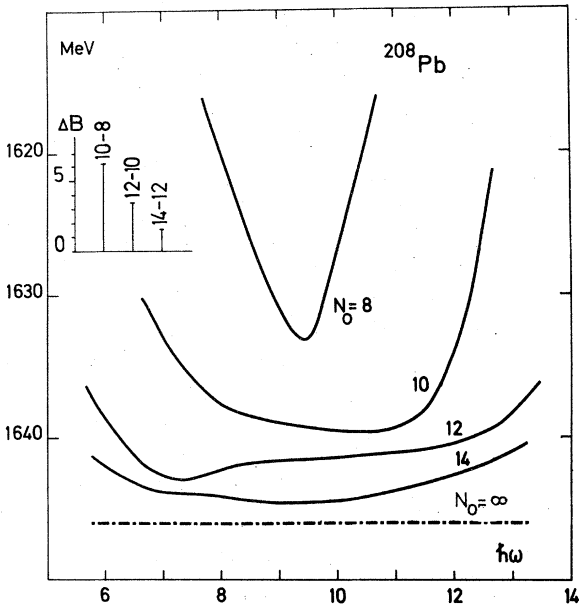

FIG. 8. The convergence rate of the HFB calculations as a function of the dimension of the HO basis.

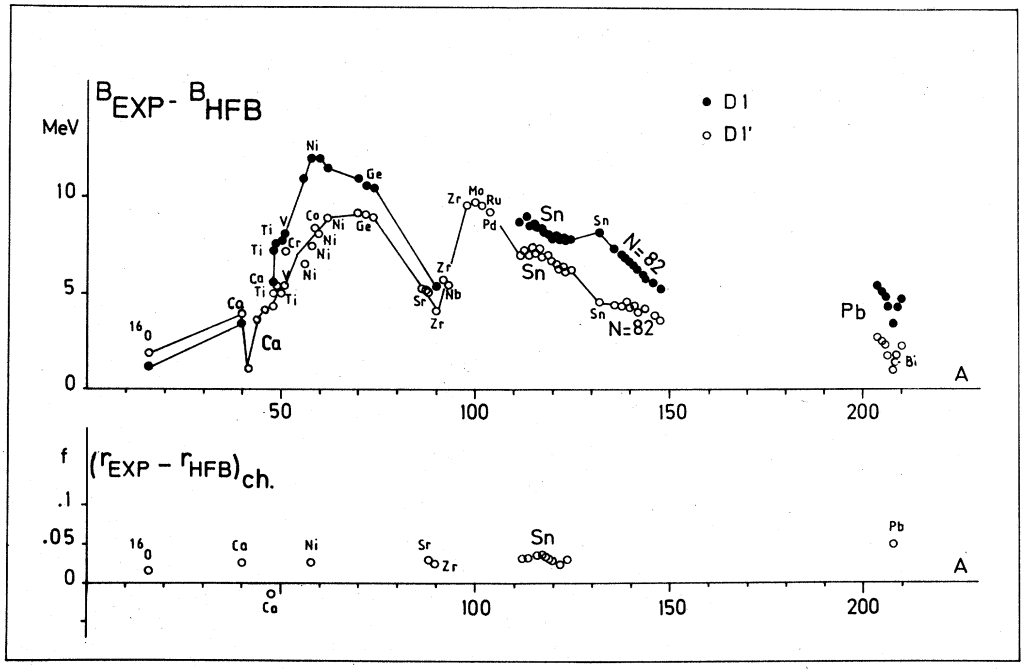

FIG. 9. Top: The total binding energy differences between the HFB results and the experimental values [A. H. Wapstra and K. Bos, Nuclear Data Tables 19, 3 (1977)]. (For a more detailed explanation see the Sec. V A.) Bottom: The differences between the HFB charge radii and the experimental values [F. Boehm, Nuclear Data Tables 14, 5-6 (1974); J. R. Ficenec *et al.*, Phys. Lett. 42B, 213 (1972)]. There is no significant difference between results obtained by $D1$ and $D1'$.

A. Total binding energies

All calculations reported here are carried out in a large basis including thirteen major shells ($N_0 = 12$), and the total energy was minimized with respect to the oscillator length parameter $b = (\hbar/m\omega)^{1/2}$. In order to check the influence of the basis truncation on the results, we studied their variation as function of the dimension (N_0) in different regions of the nuclear chart. The rate of convergence on the total binding energy is shown in Fig. 8 in the case of ^{208}Pb. In view of the regularity of the convergence, the extrapolation of the curve beyond $N_0 = 14$ seems a reasonable way to get an estimation of the difference $E(N_0 = \infty) - E(N_0 = 12)$. This difference, which is negligible for the nuclei below ^{16}O, varies almost linearly as function of the mass number to reach 3.5 MeV in the case of lead (Fig. 8). The calculated binding energies used in the discussion which follows are corrected for this truncation effect. It is worthwhile reminding that the two-body part of the center of mass motion is accounted for and the exchange part of the Coulomb field is treated exactly. The difference ΔB between the experimental total binding energies and the results of the DDHFB calculations are shown in Fig. 9 for the spherical nuclei close to the stability line. The slight differences in the variations of ΔB versus mass number for the two

TABLE VI. The 1s neutron and proton HF energy levels in some spherical nuclei. The two forces $D1$ and $D1'$ give essentially the same results. The results with the SIII interaction are from Ref. 33.

		^{16}O	^{40}Ca	^{48}Ca	^{56}Ni	^{90}Zr	^{208}Pb
SIII	n	−35.0	−44.6	−44.8	−49.6	−49.5	−50.2
	p	−31.3	−37.0	−43.0	−39.6	−40.9	−41.2
D_1'	n	−38.3	−52.1	−53.4	−58.3	−60.4	−62.4
	p	−35.0	−44.8	−51.5	−48.5	−51.4	−52.8
exp[a,b]	p	−40 ± 8	−50 ± 11	−55 ± 9		−54 ± 8	

[a] A. N. James, P. T. Andrews, P. Kirkby, and B. G. Lowe, Nucl. Phys. A138, 145 (1969).
[b] J. Mougey *et al.*, Nucl. Phys. A262, 461 (1976).

interactions come essentially from the difference in the spin orbit term. From the comparison with the experimental results, we conclude that the predictions of these DDHFB calculations are reasonable, the disagreement near closed shell nuclei being of the order of 5 MeV. The presence of oscillations in the curve reflects the fact that we have investigated also nuclei in the middle of the shells. For such nuclei the DDHFB treatment is certainly insufficient despite the fact that the pairing correlations are taken into account. For instance, if one considers the Ni or Ge isotopes these nuclei are very soft against quadrupole deformation, meaning that extra correlations should be taken into account in their description.

It is also interesting to analyze another self-consistent study[33] which aims to reproduce the experimental binding energies with different Skyrme forces. There the pairing correlations are treated phenomenologically with the BCS procedure using the pairing matrix elements of interactions which are not of the Skyrme type, the latter being inadequate for that purpose. The general trend of this calculation and ours is rather similar since both of them predict ΔB oscillating in a range of 10 MeV. The comparison is made between $D1'$ and the force SIII which is considered as the best Skyrme force in that domain. It must be pointed out that the HF field provided by our forces is much more nonlocal than by SIII, as can be seen from Table VI where the theoretical energies of the $s_{1/2}$ neutron and proton levels are listed along with the empirical estimates for the proton levels. In fact, by adjusting the parameters of the density dependence of the force, we have attempted to keep the deepest levels depressed as estimated experimentally and at the same time to get a sufficiently compressed spectrum at the Fermi surface. For fixed power of the density ($\alpha = \frac{1}{3}$) this requirement led to the upper limit of $t_0 = 1350$ fm^4. In this context it is interesting to discuss the compressibility in nuclear matter since it it closely related to the nonlocality of the HF field. As a matter of fact, the compressibility increases with decreasing nonlocality as one observes in Ref. 33. On the other hand, the situation concerning the incompressibility has been greatly clarified with the identification of the breathing mode in some spherical nuclei.[34,35] A calibration of the giant monopole resonances[28] in the framework of the RPA indicates that the incompressibility required in nuclear matter in order to reproduce the position of these resonances should be about $K = 220$ MeV. This value is very close to the compressibility of the 228 MeV obtained with our forces.

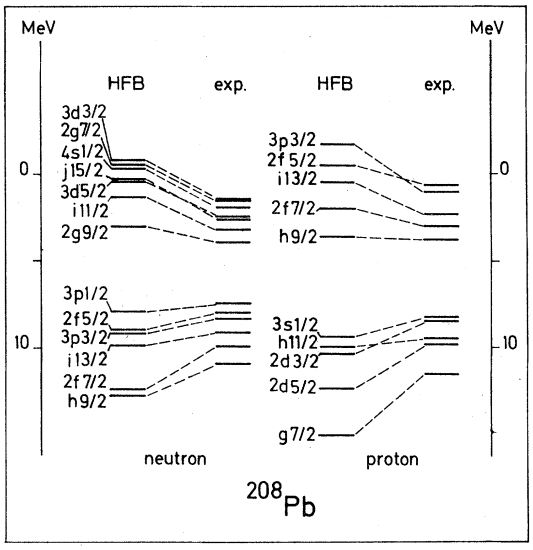

FIG. 10. The HF single particle spectrum with $D1'$ compared to the corresponding experimental values. [A. Bohr and B. Mottelson, Nuclear Structure (Benjamin, N.Y., 1969), Vol. I.]

In Fig. 10 we show the calculated HF level density in the case of ^{208}Pb compared to the empirical one. Except for an inversion of the $h_{11/2}$ and $2d_{3/2}$ protons levels the ordering of the levels is correct. On the other hand, this comparison reveals that the HF spectrum is much too dilated. However, one should bear in mind that such comparison can be only qualitative since some stray assumptions are required in order to find a simple relation between the HF spectrum and the empirical single particle energies. In particular, in our case the orbital rearrangement is nonnegligible due to explicit density dependence of the force. For instance, we calculated the difference $\Delta = {}^{209}\mathrm{B} - 2^{208}\mathrm{B} + {}^{207}\mathrm{B}$ which should be equal to $\epsilon_{p1/2} - \epsilon_{g9/2}$ in ^{208}Pb if this rearrangement were negligible. In reality we find they differ by 1.3 MeV. Furthermore, Hamamoto[36] has estimated the dynamical effects associated to the coupling of the valence particle with the core vibration. According to her results it seems important to include these effects before making a qualitative comparison even for the levels close to the Fermi surface.

B. Matter distribution and radii

The consistency of the results obtained with the HFB theory and the saturation properties of the effective forces proposed here will be emphasized in the following discussion of the relevant quantities such as neutron and proton radii and charge densities.

Figure 9 exhibits the difference between the

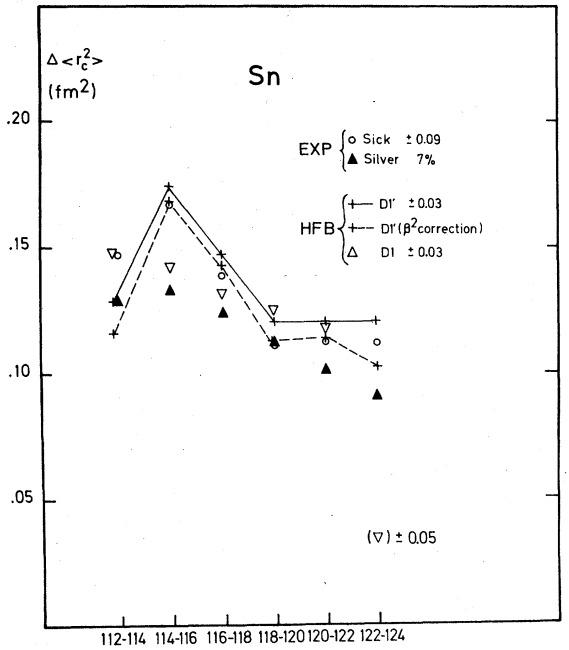

FIG. 11. The isotope shifts for the even-even tin isotopes as a function of atomic number [○–J. R. Ficenec *et al.*, Phys. Lett. 42B, 213 (1972) ▲–J. D. Silver and D. N. Stacey, Proc. R. Soc. London A332, 139 (1973)].

empirical and the theoretical charge radii for a series of spherical nuclei. The proton distribution was folded with the simple form factor:

$$f(\boldsymbol{r}) = [(a^2 - B^2)\pi]^{-3/2} e^{-r^2/(a^2-B^2)},$$

$$B = \hbar/m\omega A, \quad a = 0.65 \text{ fm},$$

in order to correct for the center of mass motion as well as to take into account the finite size of the proton. This form factor is valid for all the nuclei investigated here since the condition $B < a$ is always satisfied for $A \geq 16$. The theory predicts the charge radii with an excellent accuracy, the discrepancy with the empirical data never exceeding 1%. On the other hand, one must admit that this theory is not able to reproduce accurately some fine effects such as those observed in the isotope shifts. Like the other DDHF calculations, ours show a significant discrepancy for the isotope shift between the ^{40}Ca and ^{48}Ca ($r_p^{48} - r_p^{40} = 0.035$ as compared to -0.01 experimentally). However, by considering the neutron form factor and the electromagnetic spin orbit effects, Bertozzi *et al.*[37] have shown that the proton rms of the ^{48}Ca actually increases by 0.012 which resolves partly the discrepancy with our prediction. The rest could be probably explained by the presence of ground state correlations as explained in Ref. 33. For completeness we give in the Fig. 11 the isotope shifts for the tin. The corrections just discussed are not included except that we show the influence of the quadrupole oscillations which we have estimated with a crude model.[38] Clearly a quantitative description of the isotope shifts would require more refinement.

The recent elastic scattering experiments with high energy protons combined with the electron scattering experiments are generally considered as the most reliable source of information on the

TABLE VII. The theoretical root mean square radii of the proton and neutron distribution and their difference Δ_{n-p}. Most of the empirical values are taken from the article on proton scattering at 1 GeV by Chaumeaux, Layly, and Schaeffer (Ref. 39): (a) the authors, (b) Alkhazov, (c) Ray, (d) Negele, and (e) the most recent results by Chaumeaux and Schaeffer.

	$\langle r_p^2\rangle^{1/2}$	$\langle r_n^2\rangle^{1/2}$	Δ_{th}	Exp		
^{16}O	2.65	2.63	−0.02	−0.07[a]		
^{40}Ca	3.38	3.34	−0.04	−0.04[e]	−0.02[b]	0.01[c]
^{42}Ca	3.38	3.39	0.01	0.03[e]	0.03[b]	0.08[c]
^{44}Ca	3.39	3.45	0.06	0.02[e]	0.06[b]	0.10[c]
^{46}Ca	3.40	3.50	0.10			
^{48}Ca	3.42	3.56	0.14	0.09[e]	0.15[b]	0.19[c]
^{58}Ni	3.68	3.67	−0.01	−0.02[e]	−0.04[b]	−0.04[c]
^{90}Zr	4.18	4.24	0.06	0.05[e]	0.10[b] / 0.02	0.09[c]
^{116}Sn	4.52	4.60	0.08	0.13[d]		
^{124}Sn	4.58	4.72	0.14	0.22[d]		
^{208}Pb	5.40	5.53	0.13	0.01[b] / 0.05 / 0.02[e]	0.18[c]	

[a,b,c] From Ref. 39.

[d] J. W. Negele, Proceedings of the Conference on Modern trends in elastic electron scattering (IKO, Amsterdam, 1978), p. 73.

[e] A. Chaumeaux, R. Schaeffer (private communication).

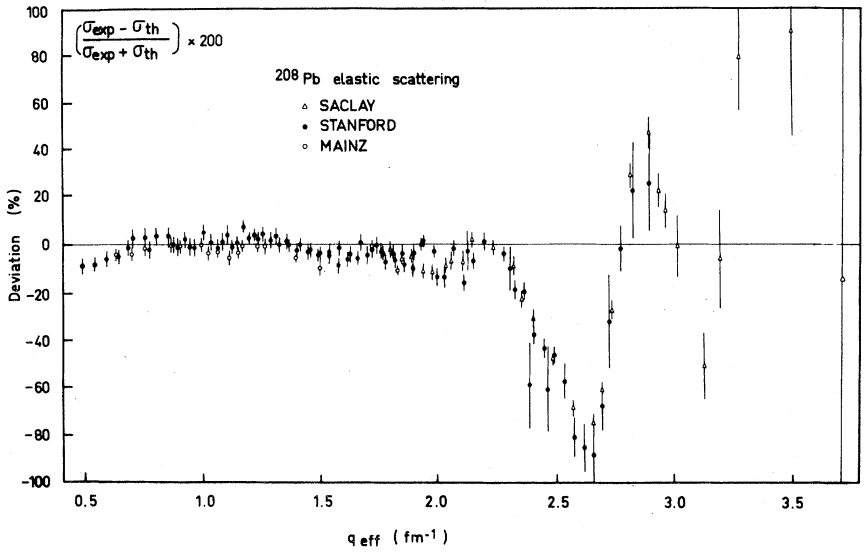

FIG. 12. The percental deviations between the calculated and the observed cross sections as a function of the momentum transfer.

neutron radii.[39] However, it must be emphasized that the analysis of the data is delicate since it involves the strong interaction and is model dependent. This remark is well illustrated by the compilation of the empirical data given in the Table VII. Looking at this compilation it becomes evident that the bulk of our HFB neutron radii falls within the experimentally established values.

The DDHFB charges densities are now compared with the ones extracted from the experiment. We chose here to restrict the discussion to the cases of ^{208}Pb and ^{58}Ni, because there exists at present a great deal of accurate data for those. In particular, the high momentum transfer experiments performed at Saclay[40,41] provided data which combined with those of Stanford and Mainz allow the determination of the proton spatial distribution very far in the interior of the nuclei. Except for a small uncertainty in the region of the central density due to the high momenta not included in the analysis, the charge density extracted from experiment can be considered as model independent. A very detailed discussion on this point can be found in Ref. 42.

First we comment on the results concerning the ^{208}Pb. Figure 12 displays the percental deviations between the calculated and the observed cross sections as function of the momentum transfer. The good agreement up to $q = 2.1$ fm^{-1} is an indication that the surface of the DDHFB density should be correct but the origin of the discrepancy at higher momenta is difficult to interpret in such a direct comparison. Thus from now on, we shall compare with the experimental densities since the very high q experiment offers this possibility. The experimental and the theoretical curves are drawn in Fig. 13 and the corresponding moments $\langle r^k \rangle^{1/k}$ are given in Table VIII. The latter give an idea of the satisfactory behavior of the theoretical density at the surface.

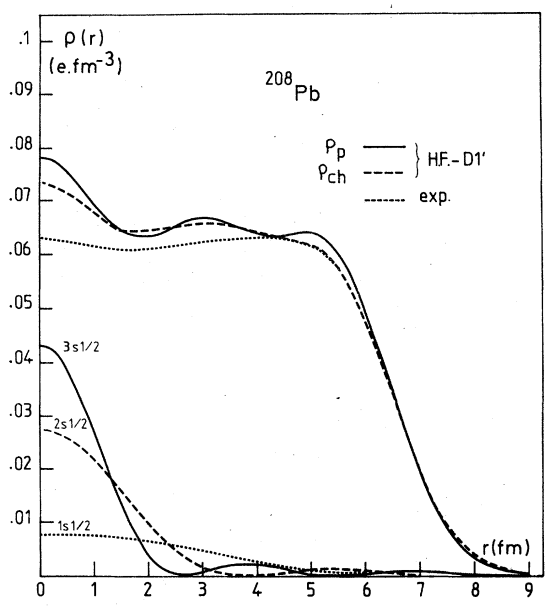

FIG. 13. The proton distribution ρ_p as well as the charge density distribution ρ_{ch} are plotted together with the density extracted from electron scattering experiment. In the lower part of the figure the contribution to the central density originating from the three $s^{1/2}$ HF states is also displayed.

TABLE VIII. The values of different moments $\langle r^k\rangle^{1/k}$ of the charge density for ^{208}Pb. The second row includes the neutron form factor. The last row corresponds to the moments of the "experimental density."

$\langle r^k\rangle^{1/k}$	$k=2$	4	6
ρ charge	5.45	5.79	6.06
ρ neut. corr.	5.43	5.77	6.03
exp	5.50	5.85	6.13

On the other hand, contrary to the experimental findings, the theory predicts large oscillations in the interior and a bump in the center of the nucleus. As seen on the same figure, the bump is due to the $3S_{1/2}$ proton level whose contribution is at least 50% of the central density. A 15% reduction of the occupation of this level would be necessary to wash out the bump. Despite the fact that the long range correlations represent a second order effect, one might hope to achieve such a reduction at least partly by including them in the description of ground state. The effect of those correlations was estimated to be weak in the case of the lead[43] but according to the authors themselves their calculation was rather qualitative. The calculation of such corrections with our RPA results[44] are in progress.

Concerning the ^{58}Ni, the interior charge density corresponding to the DDHFB solution (see Fig. 14) shows somewhat more structure than observed, but one should emphasize that the percental deviation is small, never more than about 2 or 3% even in the interior. Furthermore, the moments $\langle r^k\rangle^{1/k}$ listed in Ref. 45 demonstrate a good agreement at the surface. However, the ^{58}Ni merits special attention since it has been shown[45,46] very soft against quadrupole deformation and consequently it is not adequately described with the static DDHFB approach. Elsewhere[45] we have included in the description the dynamical effects associated to the oscillation of large amplitude. There a superposition of states of varying deformation is considered which has the desired effect of reducing the shell structure without changing the height of the central density. The fact that this correction is found rather weak can be understood by comparing the spherical density to those calculated at two very prolate and oblate deformations. For comparison we refer the reader to Ref. 46. Thus we conclude that the experimental density of the ^{58}Ni provides precious information for the spherical DDHFB calculation itself. For instance, the spherical HF calculation with the Skyrme force SIII predicts a central density which is certainly much too low (cf. Fig. 14).

C. Analysis of the magnetic electron scattering

We present preliminary results on the magnetic form factors calculated within the framework of the DDHFB theory. This is motivated by the extensive data on high magnetic multipole elastic electron scattering[47,48,49] for the series of nuclei ^{49}Ti, ^{51}V, ^{59}Co, ^{87}Sr, ^{93}Nb currently at our disposal.

First we explain briefly the way to derive the expression of the magnetic form factor with the one QP HFB state. We start with the expression

$$|F(q)|^2 = 4\pi \sum_{\lambda m\lambda} \Big| \sum_{\substack{n_\alpha n_\beta \\ l_\alpha l_\beta}} \langle n_\alpha l_\alpha j_\alpha \| T^\lambda \| n_\beta l_\beta j_\beta \rangle S^{l_\alpha j_\alpha}_{n_\alpha n_\beta}(i\lambda m_\lambda)\Big|^2 ,$$

where the reduced matrix elements are those defined by Donelly and Walecka[50] and the quantity $S^{l_\alpha j_\alpha}_{n_\alpha n_\beta}(i\lambda m_\lambda)$ is the contracted tensor defined as

$$S^{l_\alpha j_\alpha}_{n_\alpha n_\beta}(i\lambda m_\lambda) = \sum_{m_\alpha m'_\alpha} s j_\alpha \begin{pmatrix} j_\alpha & \lambda & j_\alpha \\ -m_\alpha & m_\lambda & m'_\alpha \end{pmatrix} \times \langle \tilde{0}| \eta_{i\,m+m_\lambda} a^\dagger_{n_\alpha l_\alpha j_\alpha m_\alpha} a_{n_\beta l_\alpha j_\alpha m'_\alpha} \eta^\dagger_{i m}| \tilde{0}\rangle .$$

The state $\eta^\dagger_{im}|\tilde{0}\rangle$ is the blocked HFB state which represents the ground state of the nucleus as explained in Sec. IID. Owing to the properties of the reduced matrix elements only the odd multipoles λ are to be considered so that the core does not contribute to $F(q)$. Then we can rewrite S in the form

$$S^{l_\alpha j_\alpha}_{n_\alpha n_\beta}(i\lambda m_\lambda) = \begin{pmatrix} j & \lambda & j \\ -m- m_\lambda & m_\lambda & m \end{pmatrix} \times [u^i_{n_\alpha}(l_j)u^i_{n_\beta}(l_j) + v^i_{n_\alpha}(l_j)v^i_{n_\beta}(l_j)] .$$

Inserting this expression in the definition of $F(q)$ and summing over m_λ we get the result

$$F^1(q) = \frac{4\pi}{2j+1} \sum_\lambda \Big| \sum_{n_\alpha n_\beta} \langle n_\alpha lj \| T^\lambda \| n_\beta lj\rangle [u^i_{n_\alpha}(lj)u^i_{n_\beta}(lj) + v^i_{n_\alpha}(lj)v^i_{n_\beta}(lj)]\Big|^2 .$$

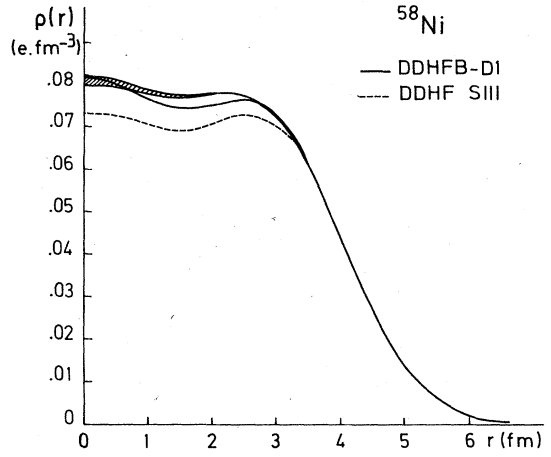

FIG. 14. The HFB charge densities of ^{58}Ni calculated with the forces $D1$ and Skyrme III. The curve with hatched part is the density extracted from the experiment (Ref. 40).

In this model the magnetic properties are determined by the blocked QP state. For vanishing pairing correlation ($u=0$) we fall back into the usual result, namely that only the valence particle contributes to the magnetic form factor. Thus the elastic magnetic electron scattering should provide a sensitive test of the single particle or QP orbit assuming that the independent QP—description is valid. In particular, in the momentum transfer range (1.7–3 fm^{-1}) at which these experiments are performed the highest multipole $\lambda=2j$ dominates and the form factor depends directly on the Fourier transform of the distribution of the valence particle. In fact, for non-vanishing pairing one checks the Fourier transform of the quantity

$$\chi(r)=\sum[u^{i}_{n_\alpha}(lj)u^{i}_{n_\beta}(lj)+v^{i}_{n_\alpha}(lj)v^{i}_{n_\beta}(lj)]\times\varphi_{n_\alpha}(r)\varphi_{n_\beta}(r)$$

rather than that of the distribution of the last QP which is given by an expression of the same form with the combination $(uu-vv)$.

The calculated form factors accounting for the nucleon magnetic and the center of mass form factors are drawn in Fig. 15 and Fig. 16. Furthermore, the contributions of highest moments to each of the magnetic form factors are given separately.

Except for the case of ^{51}V, the maximum of the form factors predicted by the theory is larger by 10 to 20%. This feature is not too surprising since corrections to the strict single quasiparticle picture due to configuration admixtures are expected to be non-negligible. In connection with the possible configuration mixings in the ground state, the spectroscopic factors obtained when trying to fit the experimental form factors with Woods-Saxon wave functions are reported in Table IX. In principle, a spectroscopic factor close to one would tend to confirm the validity of our approximation, and we observe in reality that these empirical values represent approximately the reduction factors we need to normalize the DDHFB predictions on the experimental data.

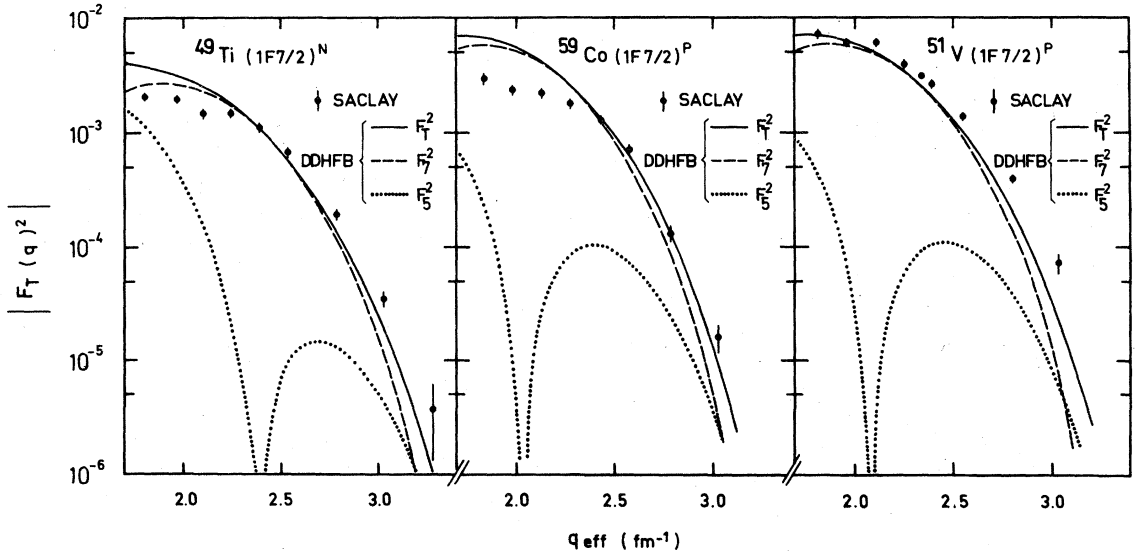

FIG. 15. The experimental results and the theoretical predictions for the magnetic form factors. The contributions of the highest magnetic moments $M5$ and $M7$ to the magnetic form factors are given separately.

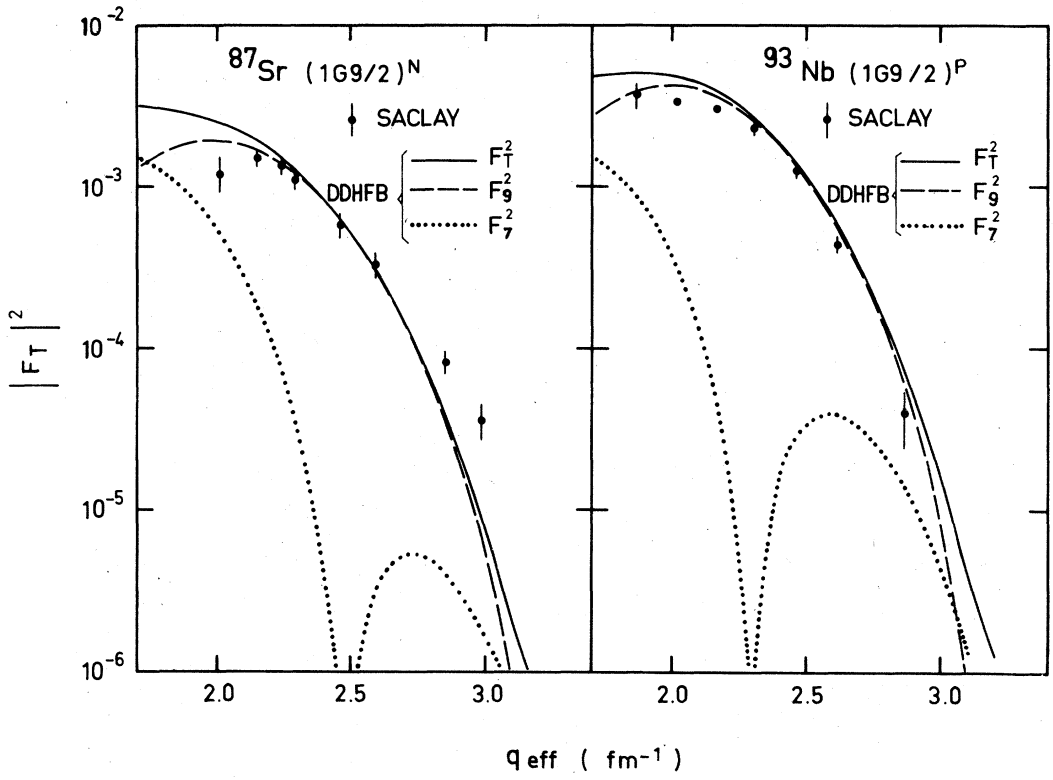

FIG. 16. The same as in Fig. 15.

A more interesting feature in this comparison concerns the behavior of the calculated form factors at the high q region. They systematically decrease more rapidly than indicated by the experiments and as consequence the rms radii of the valence nucleon radial distribution predicted by the theory are generally 2–3% greater than those extracted from the experiments (Table IX). The 8% discrepancy for the ^{59}Co will be commented later on.

In attempting to explain such descrepancy one can invoke different sources of corrections which are the following. One concerns the effect of configuration mixings on the form factors at high q. If one refers to the calculations of Suzuki *et al.*[51] and Arima[52] one should expect that the core polarization can provide a reduction of the form factors independently of the momentum transfer, i.e., without modifying their curvature. On the other side, the wave function renormalization via the particle vibration coupling might affect the high q behavior. It must be also pointed out that a perturbative estimation of the configuration mixings may be questionable for some of the nuclei in question. For instance, the ^{59}Co is a very soft nucleus as shown in Fig. 17, which suggests the presence of very deformed components in the actual ground state. Although the situation is not so crucial in the cases of ^{51}V and ^{49}Ti,[53] only the ^{93}Nb and ^{87}Sr can be considered as rigid nuclei with respect to the deformation.

Finally, another source of correction comes from the mesonic degrees of freedom. Different calculations[51,52,54] indicate a non-negligible con-

TABLE IX. The spectroscopic factors α_{SF} introduced in the fit of the magnetic cross section [see Ref. 48] and the empirical and theoretical rms radii of the valence particle density distributions.

	^{87}Sr	^{93}Nb	^{51}V	^{59}Co	^{49}Ti
α_{SF}	0.85	0.93	1.04	0.59	0.86
rms_{emp}	4.74 ± 0.04	4.89 ± 0.04	4.01 ± 0.06	4.00 ± 0.10	4.01 ± 0.03
rms_{HFB}	4.90	4.86	4.11	4.20	4.07

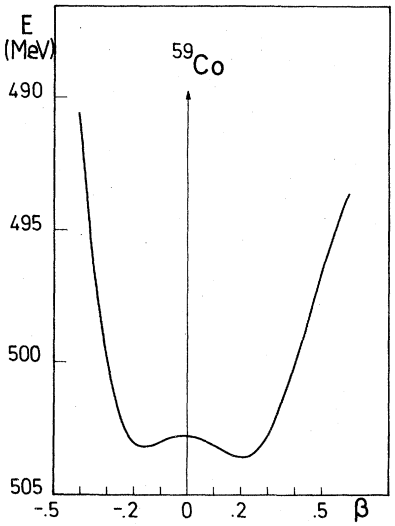

FIG. 17. Potential energy curve as a function of the deformation parameter β.

tribution from the exchange currents contributing favorably to remove the discrepancies between the DDHFB predictions and the experiments.

VI. CONCLUSION

We have thus proposed a phenomenological effective force of finite range whose parametrization is simple enough to render feasible many applications in the framework of the self-consistent approaches. It presents the following advantages.

The full nonlocality of the equations which result from the well established finite range of the effective force can be treated systematically without having recourse to any approximations, in contrast to some other approaches which overcome the difficulty by using either a very simplified force or by expanding the density matrix over the range of its nonlocality. This question is important since we are interested not only in describing the gross properties of nuclei but also the details depending on the shell model fluctuations.

This interaction seems to possess the essential characteristics necessary for the extensive applications of the self-consistent approaches. For instance, we have seen that the presence of the finite range is indispensable for deriving the most direct extension to the mean field approximation, namely the DDHFB approach. The same remarks hold true when extending the theory to the treatment of the collective excitations in the framework of the RPA, or more generally of the RPA theory developed on the quasiparticle basis. There the quasiparticle quasihole vertex function derived by expliciting the variation of the HF and the Bogolyubov fields with respect to the generalized density matrix is realistic only if it contains an effective force of nonzero range. Finally, it is likely that such effective force should be suitable for the applications using the time dependent Hartree-Fock theory.

Now, concerning the whole set of the results presented here we draw the following conclusions. First the DDHFB calculations of the finite nuclei demonstrate the possibility of describing (at the same time) the gross properties depending on the average field as well as the fine effects of the pairing correlations via the Bogolyubov field with the same force. This was achieved by fitting the force to some key experimental data with extreme care. We paid particular attention to the singlet-even component of our force. In fact, the pairing properties depend essentially on this component. This result is important since there were no *a priori* reasons that a force reproducing the bulk properties should be compatible with the pairing matrix elements.

On the other hand, the trend of the DDHFB calculations concerning the bulk properties and the pairing effect is in general very satisfactory. When significant discrepancy occurs one cannot blame systematically the DDHFB theory itself. There are two essential remarks to back this statement. In the calculations presented here we have considered very soft nuclei such as Ni and Ge and consequently we feel the necessity of going beyond the DDHFB in order to improve the description of these nuclei. Besides, even when the DDHFB can be considered as a good zero order approximation, there are nuclear properties (such as isotope shifts, central charge densities, etc.) whose accurate description depends on the details of the wave function which cannot be taken into account with an independent particle or an independent QP wave function. For instance, we shall show elsewhere that the second order corrections associated to the long range correlations (RPA) modify appreciably the interior of the charge densities.

ACKNOWLEDGMENTS

It is a pleasure to thank P. K. Kumar and Dr. R. Padjen for fruitful discussions and suggestions. We are indebted to Dr. B. Frois and his group (A. L. S. Saclay) for transmitting the electron scattering data and for stimulating various applications presented in this work. We wish to express our gratitude to R. Schaeffer

and A. Chaumeaux for communicating their most recent results extracted from high energy proton scattering.

APPENDIX A

The finite range component of our effective force has the form

$$V(r)=\sum_{i=1,2}(W+BP_\sigma-HP_\tau-MP_\sigma P_\tau)_i W_i(r),$$

where

$$W_i(r)=e^{-r^2/\mu_i{}^2}.$$

Following Talmi and de Shalit, we use the multipolar decomposition of the functions $W_i(r)$

$$W_i(r)=\sum_k W_k^i(r_1r_2)Y_k(1)Y_k(2)$$

to express the potential in the form

$$V(r)=\sum_{ksp}V_{ks}^\tau(r_1r_2)(-)^{k+s+p}\mathcal{T}_{(1)}^{(ks)p}\mathcal{T}_{(2)}^{(ks)p}. \qquad \text{(A1)}$$

The tensor $\mathcal{T}_{(1)}^{(ks)p}$ is the tensorial product of a spherical harmonic with a tensor of the spin coordinates

$$\mathcal{T}_{(1)}^{(ks)p}=[Y^k(1)\times\Sigma^s(1)]^p,\quad \Sigma^0=1,\quad \Sigma^1=\sigma,$$

and the functions $V_{ks}^\tau(r_1r_2)$ are given by

$$V_{k0}^\tau(r_1r_2)=\sum_{i=1,2}[W+B/2-(H+M/2)P_\tau]^iW_k^i(r_1r_2),$$

$$V_{k1}^\tau(r_1r_2)=\sum_{i=1,2}[(B-MP_\tau)/2]^iW_k^i(r_1r_2).$$

When using the decomposition (A1) of the potential one finds that the radial dependence of the HF and the pairing fields are determined by the two functions

$$V_{k0}^{qq'}(r_1r_2)=\sum_{i=1,2}[(W+B/2)\delta_{qq'}-(H+M/2)]^iW_k^i(r_1r_2),$$

$$V_{k1}^{qq'}(r_1r_2)=\sum_{i=1,2}[B\delta_{qq'}-M)/2]^iW_k^i(r_1r_2).$$

APPENDIX B

We examine the reduction of the geometry in the HF and the pairing fields. With the interactions of the form employed here, the geometry of the HF and pairing fields is rather simple since it is represented essentially by a squared $6j$ coefficient

$$\begin{pmatrix} l_\alpha & j_\alpha & \frac{1}{2} \\ j_\beta & l_\beta & k \end{pmatrix}^2.$$

We have eliminated this $6j$ coefficient by using the relation

$$\begin{pmatrix} l_\alpha & l_\beta & k \\ j_\beta & j_\alpha & \frac{1}{2} \end{pmatrix}^2=(-)^{j_\alpha+j_\beta+k}\sum_{s=0,1}(-)^{s+1}\hat{s}^2\begin{pmatrix} l_\alpha & l_\alpha & s \\ l_\beta & l_\beta & k \end{pmatrix}\begin{pmatrix} \frac{1}{2} & \frac{1}{2} & s \\ l_\alpha & l_\alpha & j_\alpha \end{pmatrix}\begin{pmatrix} \frac{1}{2} & \frac{1}{2} & s \\ l_\beta & l_\beta & j_\beta \end{pmatrix}$$

which allows us to get an explicit form since all $6j$ coefficients occuring in this formula are easily expressed. In fact, the $6j$ coefficients

$$\begin{pmatrix} \frac{1}{2} & \frac{1}{2} & 1 \\ l_\alpha & l_\alpha & j_\alpha \end{pmatrix}$$

and

$$\begin{pmatrix} l_\alpha & j_\alpha & 1 \\ l_\beta & j_\beta & k \end{pmatrix}$$

are directly related to the matrix elements

$$\langle(l_\alpha\tfrac{1}{2})j_\alpha|\,\overline{ls}\,|(l_\alpha\tfrac{1}{2})j_\alpha\rangle$$

and

$$\langle(l_\alpha l_\beta)k|\,\overline{l}_1\overline{l}_2\,|(l_\alpha l_\beta)k\rangle.$$

One gets

$$\begin{pmatrix} \frac{1}{2} & \frac{1}{2} & 1 \\ l_\alpha & l_\alpha & j_\alpha \end{pmatrix}=(-)^{l_\alpha+1/2+j_\alpha}\frac{\langle j_\alpha|\,\overline{ls}\,|j_\alpha\rangle}{\langle l_\alpha\|\,l\,\|l_p\rangle\langle\frac{1}{2}\|\,s\,\|\frac{1}{2}\rangle}$$

and

$$\begin{pmatrix} l_\alpha & l_\beta & k \\ j_\alpha & j_\alpha & \frac{1}{2} \end{pmatrix}^2=(-)^{l_\alpha+l_\beta+k}\times\frac{(\overline{k}-\overline{l}_\alpha-\overline{l}_\beta)}{2\hat{l}_\alpha\hat{l}_\beta\overline{l}_\alpha{}^{1/2}\overline{l}_\beta{}^{1/2}},\quad \overline{l}=l(l+1).$$

Hence the result

$$\begin{pmatrix} l_\alpha & l_\beta & k \\ j_\beta & j_\alpha & \frac{1}{2} \end{pmatrix}^2=\frac{1}{2[\hat{l}_\alpha\hat{l}_\beta]^2}\left[1+2\frac{\langle j_\alpha|\,\overline{ls}\,|j_\alpha\rangle}{\overline{l}_\alpha}\frac{\langle j_\beta|\,\overline{ls}\,|j_\beta\rangle}{\overline{l}_\beta}(\overline{l}_\alpha+\overline{l}_\beta-\overline{k})\right].$$

With this expression one exhibits clearly the one-body spin orbit contribution coming from the central component of the effective force.

APPENDIX C

We have used the following notation to define the generalized density matrix:

$$R = \begin{pmatrix} R^{11} & R^{12} \\ R^{21} & R^{22} \end{pmatrix},$$

where the objects $R^{pq}p, q = 1, 2$ are submatrices. This notation is convenient to write concisely the definition of the Bogolyubov Hamiltonian $\mathcal{H}$ or to express the relations that must satisfy a small variation of R in order to preserve the Bogolyubov conditions.

Concerning the adjustment of the Lagrange parameter λ, we recall that

$$\mathcal{H}(\lambda + \delta\lambda) = \mathcal{H}(\lambda) + \delta\lambda\hat{N}.$$

$\hat{N}$ is an operator whose representation in the original basis $(a_\alpha, a_\alpha^\dagger)$ is given by the matrix

$$N = \begin{pmatrix} I & 0 \\ 0 & -I \end{pmatrix}.$$

The linearization of the equation

$$[\mathcal{H}(\lambda) + \delta\lambda\hat{N}, R(\lambda + \delta\lambda)] = 0$$

expressed in the QP representation diagonalizing $\mathcal{H}(\lambda)$ and $R(\lambda)$ leads immediately to the expression (variation of $\mathcal{H}$ with λ is neglected)

$$(\epsilon_i + \epsilon_j)^{(1)} R_{ij}^{pq} = N_{ij}^{pq}, \quad p \neq q,$$

where the ϵ are the positive eigenvalues of $\mathcal{H}(\lambda)$. The matrix elements N_{ij}^{pq} of the operator $\hat{N}$ in the QP basis are given by

$$N_{ij}^{pq} = (B^+ N_0 B)_{ij}^{pq} = 2(UV)_{ij}.$$

Thus we obtain the expression for $\delta\lambda^q$ in the Sec. II E.

[1]J. W. Negele, Phys. Rev. C 1, 1260 (1970).
[2]J. Zofka and G. Ripka, Nucl. Phys. A168, 65 (1971).
[3]D. Vautherin and D. M. Brink, Phys. Rev. C 5, 626 (1972).
[4]X. Campi and D. W. L. Sprung, Nucl. Phys. A194, 401 (1972).
[5]H. Bethe, Annu. Rev. Nucl. Sci. 21, 93 (1971).
[6]B. H. Brandow, Ann. Phys. (N.Y.) 57, 214 (1970).
[7]K. A. Brueckner and D. T. Goldman, Phys. Rev. 117, 207 (1960).
[8]K. A. Brueckner, J. L. Gammel, and J. T. Kubis, Phys. Rev. 118, 1438 (1960).
[9]K. R. Lassey, M. R. P. Manning, and A. B. Volkov, Can. J. Phys. 51, 2522 (1973).
[10]G. Saunier and J. M. Pearson, Phys. Rev. C 1, 1353 (1970).
[11]H. S. Köhler, Nucl. Phys. A258, 301 (1976).
[12]S. A. Moszkowski, Phys. Rev. C 2, 402 (1970).
[13]H. H. Wolter, A. Faessler, and P. U. Sauer, Nucl. Phys. A167, 108 (1971).
[14]A. Banerjee, S. B. Khadhikar, and K. R. Sandhya Davi, Phys. Rev. C 7, 1010 (1973).
[15]K. Goeke, K. Allaart, H. Müther, and A. Faessler, Z. Phys. 271, 377 (1974).
[16]K. Dietrich, H. J. Mang, and J. Pradal, Phys. Rev. B22, 133 (1964).
[17]K. Kumar and M. Baranger, Nucl. Phys. A110, 529 (1968); 62, 113 (1965).
[18]A. L. Goodman, Adv. Nucl. Phys. 11, 263 (1979).
[19]J. G. Valatin, *Lectures in Theoretical Physics* (University of Colorado Press, Boulder, 1961), Vol. IV.
[20]M. Vujicic and F. Herbut, Nuovo Cimento 65B, 221 (1970).
[21]D. Gogny and R. Padjen, Nucl. Phys. A293, 365 (1977).
[22]D. Gogny, Nucl. Phys. A237, 399 (1975).
[23]K. Sugawara, Prog. Theor. Phys. 35, 44 (1966).
[24]P. Ring, H. J. Mang, and R. Beck, Z. Phys. 231, 10 (1970).
[25]D. M. Brink and E. Boeker, Nucl. Phys. 91, 1 (1967).
[26]A. B. Volkov, Nucl. Phys. 74, 33 (1965).
[27]P. J. Siemens and V. R. Pandharipande, Nucl. Phys. A173, 561 (1971).
[28]J. P. Blaizot, D. Gogny, and B. Grammaticos, Nucl. Phys. A265, 315 (1976).
[29]J. Côté and J. M. Pearson, Nucl. Phys. A304, 104 (1978).
[30]J. W. Negele and D. Vautherin, Phys. Rev. C 5, 1472 (1972).
[31]T. T. S. Kuo, E. U. Baranger, and M. Baranger, Nucl. Phys. 79, 513 (1966).
[32]R. Arvieu, E. Baranger, M. Veneroni, M. Baranger, and V. Gillet, Phys. Lett. 4, 119 (1963).
[33]M. Beiner, H. Flocard, Nguyen Van Giai, and P. Quentin, Nucl. Phys. A238, 29 (1975).
[34]N. Marty, M. Morlet, A. Willis, V. Comparat, R. Frascaria, and J. Kallne, Report No. IPNO-Ph N 75-11.
[35]D. H. Youngblood, C. M. Rozsa, J. M. Moss, D. R. Brown, and J. D. Bronson, Phys. Rev. Lett. 39, 1188 (1977).
[36]I. Hamamoto, in *Nuclear Self-Consistent Fields*, proceedings of the International Conference held at the Center for Theoretical Physics, Trieste, Italy, 1975, edited by G. Ripka and M. Porneuf (North-Holland, Amsterdam, 1975), p. 171.
[37]W. Bertozzi, J. Friar, J. Heisenberg, and J. W. Negele, Phys. Lett. 41B, 408 (1972).
[38]P. C. Reinhard and D. Drechsel, Z. Phys. A290, 85 (1979).
[39]A. Chaumeaux, V. Layly, and R. Schaeffer, Phys. Lett. 72B, 33 (1977).
[40]I. Sick *et al.*, Phys. Rev. Lett. 35, 910 (1975).

[41]B. Frois, J. B. Bellicard, J. M. Cavedon, M. Huet, P. Leconte, P. Ludeau, A. Nakada, Phan Zuan Hô, and I. Sick, Phys. Rev. Lett. 38, 152 (1977).
[42]J. M. Cavedon, Ph.D. thesis, Université de Paris Sud Centre d'Orsay, 1978.
[43]A. Faessler, S. Krewald, A. Plastino, and J. Speth, Z. Phys. A276, 91 (1976).
[44]J. P. Blaizot and D. Gogny, Nucl. Phys. A284, 429 (1977).
[45]M. Girod and D. Gogny, Phys. Lett. 64B, 5 (1976).
[46]J. W. Negele and G. Rinker, Phys. Rev. C 15, 1499 (1977).
[47]P. K. A. De Witt Huberts *et al.*, Phys. Lett. 60B, 157 (1976).
[48]I. Sick *et al.*, Phys. Rev. Lett. 38, 1259 (1977).
[49]P. K. A. De Witt Huberts *et al.*, Phys. Lett. 71B, 317 (1977).
[50]T. W. Donnely and J. D. Walecka, Nucl. Phys. A201, 81 (1973).
[51]T. Suzuki, H. Hyuga, and A. Arima, report, 1979.
[52]A. Arima, in *Proceedings of the International Conference on Nuclear Physics with Electromagnetic Interactions, Mainz, 1979* (Springer, Berlin, 1979).
[53]D. Gogny, in *Proceedings of the International Conference on Nuclear Physics with Electromagnetic Interactions, Mainz, 1979* (Springer, Berlin, 1979).
[54]J. Dubach, Phys. Lett. 81B, 124 (1979).